Universidade de Lisboa
Faculdade de Ciências
Departamento de Física

Ciências ULisboa

Electron thermal self-energy in a highly degenerate electron plasma

Mestrado em Física
Especialização em Física Nuclear e Partículas

Xavier de Sousa Ferreira Rodrigues

Dissertação orientada por:
Prof. Doutor Luís Bento

2015

To Ana,
who lives for perfection.
She found the hard way up
and takes me with her everyday.

Acknowledgements

There are definitely some people without whom, for diverse reasons, this thesis would not have been written.

Should I start in chronological order, I would firstly issue a posthumous acknowledgement to my dear mother, who, having no knowledge of Physics, has been of foremost importance to my pursuit of this area, having fed my earliest curiosity with wonderful books and endless conversations.

I would also like to thank my father for having always invested in me. It was his commitment to my education that permitted me to write this thesis today.

Thirdly, I thank my thesis supervisor, Professor Luís Bento, for having introduced me to the theme of this thesis, assisted me throughout it, and given me valuable insight into the practice of theoretical particle physics. I have learned greatly from every conversation.

At last, to my friend and wife Ana Krajinović, my gratitude is beyond any writeable scope, so I will restrict myself to a two-fold acknowledgement: for giving me all the motivation when all else was not enough; and for all the discussions, since the beginning, in which we beheld the power of knowledge, the beauty of Science and the brevity of life. Again, this work is for her.

Abstract

The aim of this work is the determination and interpretation of the energy spectrum of a highly degenerate Fermi gas of relativistic electrons. The thermal corrections to the electron's self-energy interaction are calculated to one-loop order in Quantum Electrodynamics (QED) and the resulting dispersion relation of the electron is determined.

We use the mathematical framework of finite-temperature quantum field theory, in particular the so-called real-time formalism. In the literature, this method has been applied to a symmetric plasma of massless fermions and anti-fermions at very high temperature. The electrons and positrons were shown to gain a thermal mass that is directly proportional to the coupling constant and the temperature of the plasma. Moreover, the dispersion relation was shown to yield additional solutions, interpreted as holes and anti-holes. These solutions are collective modes of the plasma and do not exist in a vacuum.

Our study of a degenerate plasma of massive electrons will show that collective plasma excitations corresponding to holes and anti-holes are also present in this system. Furthermore, we show that the electrons in the plasma acquire a thermal mass that scales with the coupling constant and the Fermi momentum of the distribution. We also found that the asymmetry of the plasma leads electrons and positrons to acquire a thermal mass that is different from each other, with the difference given approximately by the free electron mass m_e. The same difference was found for holes and anti-holes.

The importance of this study resides in its potential application to several astrophysical systems where a degenerate distribution of relativistic electrons is present, such as the core of supernovae during their collapse, and the core of compact stars. A thermal correction to the electron and positron mass could yield relevant changes to the kinetics of reactions such as (inverse-)β decay, and therefore to the rates of electron production and absorption. This may alter the conditions for chemical equilibrium as well as the rate of neutrino emission associated with these processes.

Resumo

O presente trabalho tem como objetivo a determinação e interpretação física do espetro energético de um gás de Fermi degenerado de eletrões, no regime relativista. Para isso, estudam-se os efeitos do banho térmico sobre a interação de auto-energia de um eletrão em segunda ordem em Eletrodinâmica Quântica (QED) e calcula-se a resultante relação de dispersão do eletrão no banho térmico.

A auto-energia é uma correção relativista à energia do eletrão, que advém da sua emissão e reabsorção de fotões virtuais no curso da sua propagação. No vácuo, a correção da auto-energia à carga e massa do eletrão apresenta uma divergência ultra-violeta; para obter resultados físicos é necessário proceder à regularização do integral, depois da qual a massa e a carga devem ser renormalizadas de modo a corresponderem às propriedades observáveis do eletrão.

Ao propagar-se num meio físico, um eletrão vai interagir com a distribuição de partículas que constitui o meio. Isto irá levar a uma correção térmica à auto-energia que, no geral, vai alterar a relação de dispersão do eletrão. Para calcular este efeito é necessário considerar a estatística da distribuição; para tal, iremos usar métodos de teoria quântica do campo a temperatura finita, em particular o chamado formalismo de tempo real, que consiste em adicionar ao propagador uma componente térmica resultante da presença dos eletrões e/ou positrões do plasma, componente essa que tem que ser pesada estatisticamente tendo em conta a distribuição de Fermi-Dirac das partículas do banho térmico. Isto irá introduzir no propagador uma dependência das variáveis termodinâmicas do banho, tais como o momento de Fermi (no caso de uma distribuição degenerada), a densidade de partículas, a temperatura, etc. Ao incluir este 'propagador térmico' no cálculo da auto-energia do eletrão, a relação de dispersão (que corresponde aos polos do propagador) irá então sofrer a correção térmica referida, que dependerá portanto das variáveis termodinâmicas. Para além disso, a presença do plasma vai introduzir na descrição da auto-energia uma dependência do referencial de repouso do plasma, o que irá quebrar a invariância de Lorentz que é característica da auto-energia no vácuo. Concretamente, a auto-energia do eletrão no meio irá depender das componentes da energia-momento do eletrão p_0 e $|\mathbf{p}|$, ao contrário do caso da sua propagação no vácuo, em que a auto-energia pode apenas depender do invariante de Lorentz $p^2 = p_0^2 - \mathbf{p}^2$.

Damos igualmente uma interpretação física do processo de auto-energia num meio térmico. Mostramos que a correção térmica à auto-energia advém da possibilidade de o fotão virtual emitido pelo eletrão ser absorvido não por si próprio, mas por um eletrão ou positrão do meio, cuja energia é dada estatisticamente pela distribuição de Fermi-Dirac.

Um estudo semelhante foi conduzido por H. A. Weldon para o caso de um plasma simétrico de fermiões e anti-fermiões sem massa, no regime de alta temperatura. Weldon mostrou que a correção térmica à auto-energia confere aos fermiões uma massa em repouso efetiva, a que podemos chamar massa térmica, que é diretamente proporcional à temperatura do plasma e à constante de acoplamento da teoria. Um outro resultado relevante do referido estudo foi a existência de quatro soluções da relação de dispersão do eletrão, em vez das duas encontradas no vácuo correspondentes à propagação de um fermião e de um anti-fermião. Mostrou-se que para além das duas soluções correspondentes ao fermião e anti-fermião termalizados, as duas soluções adicionais têm as propriedades correspondentes a excitações de lacuna e anti-lacuna. Em particular, a relação entre quiralidade e helicidade destas soluções é a oposta do fermião e anti-fermião: enquanto que estas últimas, no limite de massa nula, apresentam igual valor próprio de quiralidade e helicidade, a lacuna e anti-lacuna têm quiralidade oposta à helicidade.

Com o presente estudo pretende-se aplicar semelhante formalismo a um plasma altamente degenerado de eletrões massivos, no contexto da QED. Este sistema apresenta, por um lado, uma violação da quiralidade, introduzida pela massa finita dos eletrões, e por outro, uma assimetria entre partículas e anti-partículas devida à inexistência de positrões no banho térmico. Ambas estas características estavam ausentes no sistema estudado por Weldon e iremos observar que têm efeitos na relação de dispersão que não se observavam no caso estudado pelo autor.

A relação de dispersão exata do eletrão é calculada sob a forma implícita, e apresenta-se graficamente o resultado numérico para um plasma com momento de Fermi $p_F = 200\, m_e$, onde m_e é a massa do eletrão. Este valor é representativo da distribuição degenerada de eletrões presente no núcleo de uma estrela de neutrões, que se tomará como exemplo. Os resultados mostram a existência de uma massa térmica das soluções de eletrão e positrão, que escala com o momento de Fermi do plasma e com a constante de acoplamento. Observa-se também a presença de soluções de lacuna e anti-lacuna, tais como observadas na literatura.

Para cada uma das quatro excitações do sistema obteve-se uma expressão aproximada da sua massa térmica. Uma das características observadas é a existência de uma diferença entre as massas térmicas do eletrão e da lacuna; mostrou-se que esta diferença é dada aproximadamente pela massa do eletrão, m_e. Esta característica é portanto exclusiva de plasmas massivos, e de facto não está presente nos resultados da literatura referida acima. Outra característica obtida na nossa análise é o facto de que as relações de dispersão obtidas para o eletrão e para o positrão são diferentes neste sistema, assim como as relações de dispersão de lacuna e anti-lacuna. Esta propriedade provém da assimetria entre matéria e anti-matéria do banho térmico, que contém apenas eletrões e não positrões; de facto, este resultado não foi observado por Weldon para o caso de um plasma simétrico de eletrões e positrões, o que se justifica pelo facto de nesse sistema, a simetria entre matéria e anti-matéria presente no vácuo estar presente também no interior do plasma.

Para além da comparação qualitativa entre os nossos resultados e aqueles obtidos na literatura, procede-se também a uma comparação quantitativa da massa térmica obtida em ambos os casos, com o intuito de contribuir para uma validação dos nossos resultados. Para tal, fazem-se as adaptações necessárias a uma comparação direta; nomeadamente, considera-se a presença adicional de uma distribuição de positrões com igual momento de Fermi, de modo a conferir simetria ao banho térmico, e adicionalmente toma-se o limite $m_e \to 0$, que foi o caso estudado por Weldon. Observa-se um acordo entre as expressões obtidas e os resultados da literatura, para plasmas da mesma densidade.

Os resultados obtidos poderão ser relevantes para o estudo de certos sistemas astrofísicos contendo distribuições degeneradas de eletrões. Este é o caso, por exemplo, do núcleo de uma supernova tipo II, que a partir da explosão colapsa abruptamente, dando eventualmente origem a uma estrela compacta, por exemplo uma estrela de neutrões. Durante o colapso, ocorre uma gradual compressão do material estelar; a determinada altura, este processo levará à degenerescência do gás de eletrões. Um gás degenerado de eletrões também está presente na fase ulterior de estrela de neutrões. Durante o colapso, assim como no interior da estrela de neutrões, ocorrem o decaimento β e β inverso, cujas taxas influenciam o equilíbrio químico entre protões, neutrões e eletrões. A existência de uma massa térmica do eletrão e positrão poderá afetar a cinemática destes processos e assim as suas taxas de decaimento. Por sua vez, isso poderá alterar as condições de equilíbrio no material estelar. Ao mesmo tempo, poderá também alterar a taxa de emissão de neutrinos e anti-neutrinos, que são produzidos em quantidades copiosas nestes corpos, principalmente durante a explosão das supernovas.

Contents

Chapter 1

Introduction

In quantum field theory, particle interaction is made possible by the local coupling of the quantum fields. The 'strength' of the coupling is given by a coupling constant dependent on the theory and, in the case of some theories, on the energy scale of the interaction. In Quantum Electrodynamics (QED), the coupling between the electron and photon fields is weak, since the coupling constant is the elementary charge e, which is very small – in the natural unit system[1] employed throughout this work, $e^2 = 4\pi\alpha = 4\pi/137$, where α is the fine structure constant. Because of the weakness of the electromagnetic coupling, interactions in QED may be treated as a small perturbation to the corresponding free-field system.

This thesis focuses on the effects of a physical medium on the dispersion relation of a propagating electron. In particular, two media will be discussed: a plasma of electrons and positrons, and a plasma of ions and electrons (see further below). We will study the effect of what would be called the 'exchange' interaction in the non-relativistic Hartree-Fock theory [1] – by exchange of a photon, two electrons with the same spin acquire each other's energy-momentum, i.e. they swap states. In QED, this process is of order e^2 because of the coupling of the exchanged photon to both electrons.

A mathematical framework suitable for including the thermodynamic effects of the medium while retaining the quantum field-theoretical treatment of particles is so-called *thermal* (or *finite-temperature*) field theory. A formalism of this sort was first used in the mid-1950s in a non-relativistic context for a description of condensed matter systems, where the energy scale is typically very low. In 1955, for instance, T. Matsubara devised a method of calculating the partition function of the electron-phonon system based solely on methods of quantum field theory [2]. In 1965, thermal field theory emerged

[1] $\hbar = c = k_B = 1$, where $\hbar$ is the reduced Planck constant, c is the speed of light in a vacuum and k_B is the Boltzmann constant.

in its relativistic form in a paper by Fradkin [3] where the partition function of a relativistic system was determined by means of a propagator formalism. Nowadays, two particular methods are generally used to perform thermal field theory: the *imaginary*- and *real*-time formalisms [4, 5]; in the present work, the latter method will be used. In a nutshell, this consists of adding to the 'zero-temperature' propagator (i.e. prescribed by conventional QED in a vacuum), a term representing the contribution from the real particles making up the plasma. This contribution must of course be integrated over the energy distribution of the particles, which in turn depends on state variables such as temperature, Fermi energy (in the case of a degenerate system), density, etc. In this manner the thermodynamics of the medium is incorporated in the theory.

As will be shown, in finite-temperature QED the electron exchange interaction mentioned above may be calculated as a 'thermal self-energy' correction. In zero-temperature QED the self-energy is a radiative correction to the energy of an electron propagating through the vacuum that arises when we consider the possibility of emission and re-absorption of virtual photons by the electron. In particular, the second-order term in the perturbative expansion of the self-energy involves the emission and re-absorption of only one virtual photon. Because the self-energy stems from the intrinsic quantum fluctuations of the vacuum, all electrons are subject to this phenomenon, and therefore the effective mass obtained by this correction is in fact the observed electron mass. This equivalence is achieved in QED by performing the regularisation of the self-energy integral (which would otherwise be divergent), followed by renormalisation of the regularised mass parameter [6]. However, at finite temperature the self-energy will include a term accounting for the possibility that the emitted photon, rather than reabsorbed by the electron, is absorbed by another particle of the plasma (be it another electron or a positron). This will yield a momentum-dependent correction to the energy of the electron.

The method described above for the calculation of the thermal self-energy correction was first applied by Weldon [7–9] to the case of a symmetric, chirally invariant plasma (i.e. with the same number of fermions and anti-fermions, and all particles considered massless[2]), in the very high temperature regime. Note that in a classical thermodynamic system an increase in temperature would lead to an expansion of the system due to the higher average particle momentum, therefore becoming increasingly less dense, which would ultimately annihilate the effects of a collective interaction. However, in a relativistic quantum system at high temperature there is enough energy for the creation of large amounts of particle-antiparticle pairs. As a consequence, particle density will

[2] At low temperatures, chiral symmetry is broken by the finite masses of the fermions in the theory; however, above a certain temperature T_χ chiral symmetry will be restored exactly, and the fermions will behave as if they were massless [10].

increase with temperature and the effect of the medium will become more significant. It was found that the presence of the plasma yields for a massless fermion a 'thermal' rest mass, i.e. a minimum value of energy inside the plasma, which depends linearly on the coupling constant and on the temperature of the plasma. This is the fermionic equivalent to the so-called 'plasma frequency', the finite rest energy acquired by gauge bosons in a plasma [11]. Furthermore, these corrections were shown to cause additional fermionic solutions of the dispersion relation apart from the thermalised electron and positron. These modes are collective excitations of the plasma and do not exist in a vacuum. Weldon, as well as other authors subsequently, have interpreted these solutions as *hole* and *anti-hole* excitations, also called *plasminos* and *anti-plasminos* [8, 12]. An interpretation of these modes will be presented through an analysis of their spinorial structure.

One of the interesting applications of these results is the Quark-Gluon Plasma (QGP), a hypothetical state of matter predicted by Quantum Chromodynamics (QCD). It has been shown that in this theory the confinement of quarks in hadrons only occurs below a certain value of temperature, possibly around 150-200 MeV [13]. Above the deconfinement temperature hadronic matter cannot exist; rather, quarks have freedom at long-distance range. In order to study this new state of matter, an extensive experimental program was initiated in experiments such as LHC where high-energy ion collisions are expected to yield droplets of quark matter sufficiently hot and dense for the QGP to form [14]. The results obtained by Weldon may then be applied as a test to the presence of the QGP, particularly the observation of hole states, that have rather different behaviour from quarks and anti-quarks. One of the major motivations for the discovery and manipulation of the QGP is the early Universe. Namely, hadronic confinement must have only become possible after around 10 μs from the Big Bang [15]; if the transition from the QGP to hadronic matter was a first order phase transition, it has probabily created inhomogeneities in the baryon density that may have subsisted until the age of nucleosynthesis, thus altering the abundances of the elements [4, 15].

The main objective of this work is the determination of the thermal self-energy correction for the case of a relativistic plasma of massive electrons in the zero-temperature approximation. This will allow for a calculation of the electron dispersion relation and thus the excitation spectrum of the system.

At zero temperature particles have the least possible momentum; however, because of Pauli's exclusion principle electrons of the plasma are forced to occupy states with momenta up to the Fermi energy (this is the so-called degeneracy pressure, or Fermi pressure). For systems with high density, the Fermi energy will be very large and thus a relativistic treatment will be required. As we shall see, the presence of the medium will increase the electron rest mass by an mount that scales with the coupling constant and the Fermi momentum. Moreover, the dispersion relation will yield additional solutions corresponding to (anti-)hole states, like in the case of a high-temperature symmetric plasma. However, one fundamental difference we will find is that the rest mass of (anti-)hole excitations will differ from that of electrons; besides, we will find the dispersion relation of electrons to be different from that of positrons and likewise for holes and anti-holes. This feature is a consequence of the asymmetry of the plasma.

The results obtained in the present work may have future applications in astrophysical systems that contain a degenerate distribution of electrons at very high density. One application of particular interest is the explosion of core-collapse supernovae and subsequent formation of compact stars [16]. This happens at the end of the life of stars with more than around eight solar masses (if the star is not massive enough to form a black hole). During the collapse of the supernova core the density increases very rapidly. This promotes electron capture by protons to form neutrons (with the release of a neutrino, which eventually escapes the core, leading to its gradual cooling [16]). This reaction therefore starts dominating over electron emission, until chemical equilibrium is reached [17]. At this point, the electron distribution is degenerate. A thermal mass of the electrons such as that found in the present study would change the kinematics of electron emission and absorption, thereby changing the rate of either process and potentially modifying the conditions for equilibrium. Moreover, the neutronp and anti-neutrino production rates may also be affected. Such astrophysical applications would be most interesting topics for future investigation.

1.1 Overview

A brief survey of the self-energy in zero-temperature QED is presented in Chap. 2.

In Chap. 3 we introduce the necessary tools for performing quantum field theory at finite temperature, starting with concepts from quantum statistcal physics and understanding how they are included in the QED propagators by means of real-time formalism. In the end of the chapter, the thermal propagator of the electron is derived, which underlies the mathematical formalism throughout the rest of the thesis.

Chap. 4 introduces the self-energy calculations using as an example H. A. Weldon's work regarding a chirally invariant, symmetric plasma in the high-temperature regime [7, 8], followed by an interpretation of the results.

Chap. 5 presents the main analysis of this work – the study of the self-energy of a massive electron in a highly degenerate medium. We start with a description of some physical properties of such system, followed by a our results and their discussion. These include the dispersion relation of the electron and the (anti-)hole solutions and in particular their thermal rest masses. Finally, the results will be compared with the high-temperature case discussed in Chap. 4.

The thesis will conclude in Chap. 6 with a summary of the main results and an outlook to possible future research.

Chapter 2

Electron self-energy in a vacuum

In this chapter we shall introduce the concept of the self-energy of an electron in a vacuum. This phenomenon will underlie all the present work, and in successive chapters will be adapted to a finite-temperature formalism.

2.1 Single-particle propagators

Any field theory begins with the prescription of a Hamiltonian (or equivalently a Lagrangian, the Hamiltonian however being more useful to the present discussion). In particular, QED may be built upon the following Hamiltonian [6]:

$$\hat{H} \;=\; \hat{H}^0 + \hat{H}^{\text{int}} \tag{2.1}$$

where $\hat{H}^0$ is the term accounting for the kinetic energies of the free electron and electromagnetic fields (with no interactions), while $\hat{H}^{\text{int}}$ accounts for the electromagnetic interaction,

$$\begin{aligned}\hat{H}^0 &= \hat{H}^0_e + \hat{H}^0_{EM} \\ &= \int d^3\mathbf{x}\;\; \bar{\psi}(x)\big(-i\boldsymbol{\gamma}\cdot\nabla + m\big)\psi(x) + \frac{1}{2}\int d^3\mathbf{x}\big[\boldsymbol{E}^2(x) - \boldsymbol{B}^2(x)\big], \qquad (2.2\text{a}) \\ \hat{H}^{\text{int}} &= e\int d^4x\big[\bar{\psi}(x)\gamma^\mu\psi(x)\big]\cdot A_\mu(x), \qquad (2.2\text{b})\end{aligned}$$

where $\boldsymbol{\gamma}$ is a 3-component object comprising the Dirac matrices γ^i, A^μ is the electromagnetic 4-potential, ψ is a quantised fermionic field in the interaction representation, and $\bar{\psi} = \psi^\dagger\gamma^0$. As mentioned in the introduction, e is the elementary charge, that acts as the coupling constant in the theory. Throughout this thesis m will represent the electron mass.

Let us recall the meaning in practice of the Heisenberg and interaction representations, while referring the reader to any textbook on field theory for a detailed explanation [1, 6, 18]: fields in the Heisenberg representation have time evolution dependent on the full Hamiltonian of the system, i.e. [1]

$$\psi_H(x) \;=\; e^{i\hat{H}t}\psi_S(\mathbf{x})e^{-i\hat{H}t}, \tag{2.3}$$

where $\psi_S(\mathbf{x})$ is a static field operator, given by $\psi_S(\mathbf{x}) = \psi_H(0,\mathbf{x})$, which we refer to as being in the Schrödinger representation. From (2.3) it follows immediately the differential equation expressing the operator's time evolution,

$$\frac{\partial}{\partial t}\psi(x) \;=\; i[\hat{H},\psi(x)]. \tag{2.4}$$

Finally, we note that in the Heisenberg representation the states are time-independent: $|\Psi\rangle_H = \big|\Psi(\mathbf{x})\big\rangle_H$.

In the interaction representation, however, both fields and states are time dependent. This representation can be used only for systems whose Hamiltonians are separable into free and interaction contributions, as is the case of the QED Hamiltonian (2.1). The evolution of operators and states in the interaction representation is as follows [1] (since we will make consistent use of the interaction representation throughout this work, we will not use any subscript such as ψ_I, etc., unlike the other representations, which will allways be identified)

$$\frac{\partial}{\partial t}\psi(x) \;= i[\hat{H}_0,\psi(x)], \tag{2.5a}$$

$$i\frac{d}{dt}\,|\Psi\rangle \;= \left(e^{i\hat{H}_0 t}\hat{H}^{\mathrm{int}}e^{-i\hat{H}_0 t}\right)|\Psi\rangle \tag{2.5b}$$

Result (2.5a) shows that operators in the interaction representation evolve according to the *free* Hamiltonian of the system, which means that all the effects of the interactions are contained within the states $|\Psi\rangle$. This is, indeed, the major advantage of the interaction representation, and the reason of its usefulness in field theory.

This means that any field in the interaction representation, even pertaining to a system with interactions, will be solution of the equation of motion of a noninteracting particle. In the case of the electron field this is Dirac's equation:

$$(i\partial\!\!\!/ - m)\psi \;=\; 0, \tag{2.6}$$

where we have used Feynman's slash notation $\partial\!\!\!/ = \partial_\mu \gamma^\mu$. In the interaction representation *any* fermionic field $\psi(x)$ is a solution of Dirac's equation. Such free particle solutions have a well known form, namely [6]:

$$\begin{aligned} \psi(x) &= \sum_s \int \frac{d^3p}{(2\pi)^3 2E_p} \left(b_s(p) u_s(p) e^{-ip\cdot x} + d_s^\dagger(p) v_s(p) e^{ip\cdot x} \right) \\ \bar{\psi}(x) &= \sum_s \int \frac{d^3p}{(2\pi)^3 2E_p} \left(b_s^\dagger(p) \bar{u}_s(p) e^{-ip\cdot x} + d_s(p) \bar{v}_s(p) e^{ip\cdot x} \right), \end{aligned} \tag{2.7}$$

where $E_p \equiv E(|\mathbf{p}|) = \sqrt{\mathbf{p}^2 + m^2}$, operator $b(^\dagger)$ destroys (creates) a fermion with 4-momentum p, $d(^\dagger)$ destroys (creates) an antifermion, and $u_s(v_s)$ is the spinor of an (anti)fermion with spin s.

Let us first use the Heisenberg representation in order to write the *exact single-electron propagator*, which we define to be the following expectation value[1]:

$$S(x, x') \;=\; -i \left\langle 0 \middle| T\big[\psi_H(x)\bar{\psi}_H(x')\big] \middle| 0 \right\rangle_H \tag{2.8}$$

where we have used the subscript H to indicate the Heisenberg representation of the fields as well as the ground state. Also, we have used the time-ordering operator T, which arranges any number of terms 'chronologically' (i.e. with decreasing values of time variable):

$$T\big[\psi(t)\bar{\psi}(t')\big] \;=\; \theta(t - t')\psi(x)\bar{\psi}(x') - \theta(t' - t)\bar{\psi}^\top(x')\psi^\top(x) \tag{2.9}$$

(the minus sign on the second term is due to the permutation of two fermionic fields.)

[1]For simplicity, we will suppress the spinorial indices $\alpha\beta$ in the fields, as well as in the propagators ($S \equiv S^{\alpha\beta}$).

We cannot calculate the propagator (2.8) exactly insofar as we are ignorant of the expression of the fields ψ_H,$\bar{\psi}_H$, which, as discussed above, include the electromagnetic interaction. What we can calculate, however, is the propagator of a *non-interacting* system, which may be done by using the interaction representation, wherein the fields have the free particle expression (2.7). We may then write the *free particle propagator* using both fields and ground state in the interaction representation:

$$S^0(x,x') \;=\; -i\left\langle 0\left| T\left[\psi(x)\bar{\psi}(x')\right] \right| 0\right\rangle . \tag{2.10}$$

Note that all effects of the electromagnetic interaction were absorbed into the new definition of the ground state, which will not concern us. The free electron propagator has been calculated in appendix A in momentum space (which can be done for an isotropic, homogeneous system), yielding

$$S^0(p) \;=\; \frac{1}{\not p - m + i\epsilon} \;=\; \frac{\not p + m}{p^2 - m^2 + i\epsilon}, \tag{2.11}$$

that bears the celebrated name of Feynman propagator.

We notice right away one major feature of the propagator – its poles (that is to say, the zeros of the denominator) yield the solutions to Dirac's equation (2.6):

$$\begin{aligned} p^2 - m^2 &= 0 \\ \Longrightarrow\; p_0^2 &= \mathbf{p}^2 + m^2 \\ \Longrightarrow\; p_0 &= \pm\, E_p. \end{aligned} \tag{2.12}$$

As for the *exact* propagator, which is the solution when the electromagnetic interaction is accounted for, it must be calculated perturbatively, that is, considering the electromagnetic interaction as a small perturbation to the free ('unperturbed') system described by $\hat{H}^0$. The overall procedure of the perturbative expansion, leading to Feynman's rules, is briefly explained in appendix B; to our present discussion, it will suffice to state that the perturbative expansion implies the sum of Feynman diagrams to all orders, and each of these diagrams involves only the *free propagator* S^0 (drawn as an internal straight line), and the free photon propagator,

$$D^0_{\mu\nu}(k) \;=\; \frac{-ig_{\mu\nu}}{k^2 + i\epsilon}, \tag{2.13}$$

represented an internal curvy line. To second order in the perturbative expansion (no first-order terms contribte to the single-particle propagator), only *two* topologically different diagrams arise (again, we refer to appendix B for the rationale)

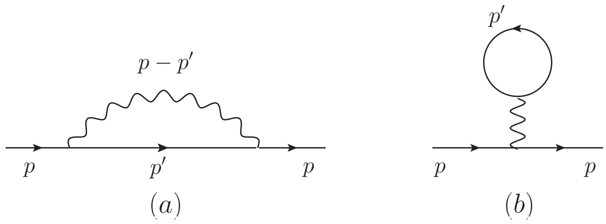

FIGURE 2.1: Second-order diagrams that arise in the expansion of the electron propagator. (a) Electron self-energy diagram. (b) Tadpole diagram.

Figure 2.1(a) is called a *self-energy* diagram and represents the self-interaction of the propagating electron through the emission and absorption of a virtual photon. *Virtual*, of course, means the photon needs not obey the real photon dispersion relation $\omega = k$. The same happens for the internal fermionic line, which represents a virtual electron, i.e. with $p_0 \neq \sqrt{p^2 + m^2}$.

Figure 2.1(b), on the other hand, is often called a *tadpole* diagram and it may be shown after integration to yield zero contribution to the propagator in a vacuum [6]. For reasons that will become apparent in §4.2, tadpole-type diagrams also do not contribute to the study of neuter systems at finite temperature. As such, in our study we will only need to care for the self-energy contributions.

2.2 The electron self-energy

It is clear that in the self-energy diagram of fig. 2.1, any value of the energy-momentum $p' = (p'_0, \mathbf{p}')$ will satisfy energy-momentum conservation, because the photon is defined as carrying the difference between that and the energy-momentum p of the real electron. So all values of p'_0 and $\mathbf{p}'$ will contribute to the overall amplitude; the rules of quantum mechanics instruct us to add such contributions, so that we must integrate over this unknown energy and momentum [18] – this is effectively one of the Feynman rules for the evaluation of the diagrams. The amplitude of the self-energy diagrams may then be written [6]

$$\mathcal{M} = \bar{u}_s(\mathbf{p})\Sigma(p)u_s(\mathbf{p}) \tag{2.14}$$

where the spinors simply proceed from the external lines of the diagram, and the *electron self-energy* $\Sigma(p)$ is the result of the integration of the free propagators of the loop [cf. fig. 2.1(a)]:

$$\begin{aligned}\Sigma(p) &= e^2 \int \frac{d^4p'}{(2\pi)^4} D^0_{\mu\nu}(p-p')\gamma^\mu S^0(p')\gamma^\nu \\ &= e^2 \int \frac{d^4p'}{(2\pi)^4} \left(\frac{-ig_{\mu\nu}}{(p-p')^2+i\epsilon}\right)\gamma^\mu \left(\frac{\not{p}'+m}{(p-k)^2-m^2+i\epsilon}\right)\gamma^\nu \\ &= -ie^2 \int \frac{d^4p'}{(2\pi)^4} \frac{\gamma^\mu(\not{p}'+m)\gamma_\mu}{(p'^2-m^2+i\epsilon)[(p-p')^2+i\epsilon]} \end{aligned} \tag{2.15}$$

Notice that the self-energy Σ is a 4×4 matrix whose elements have units of energy depend solely on the electron's energy-momentum p.

2.3 The dressed propagator

Let us now consider, for any $2n$-th order in the perturbative expansion, the series of diagrams with n insertions of the Σ-loop along the electron propagator:

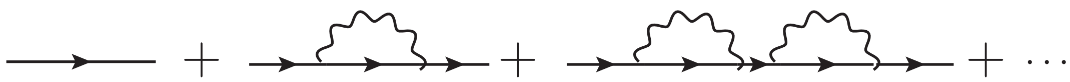

FIGURE 2.2: Representation of the Dyson series yielding the dressed electron propagator.

We see that each diagram of successively higher order may be built from the previous one by adding a proper self-energy of second order Σ, connected to a free electron propagator S^0. The sum of these contributions to all orders is called Dyson's series and may then be written as

$$\begin{aligned}S(p) &= S^0(p)\sum_{n=0}^{\infty}\left[\Sigma(p)S^0(p)\right]^n \\ &= S^0(p)\left(1-\Sigma(p)S^0(p)\right)^{-1},\end{aligned} \tag{2.16}$$

where the latter expression follows from the realisation that this is just a geometric series with 'ratio' $\Sigma(p)S^0(p)$. From it, and given the form of S^0 (2.11), one immediately obtains

$$S(p) \;=\; \frac{1}{\not{p} - m - \Sigma(p) + i\epsilon}, \tag{2.17}$$

which bears the name of *dressed propagator*. It is the exact contribution to the propagator, to all orders, of the electron's self-energy phenomenon. This is the propagator that will interest us in the present work.

As we have seen, the only four-vector upon which $\Sigma(p)$ depends (since the components of k are integrated away) is p (cf. (2.15)). Therefore, it must bear the structure [6]

$$\Sigma(p) \;=\; A\not{p} + Bm, \tag{2.18}$$

A and B being scalars, and therefore dependent only on p^2. In Chap. 4 we will see that (2.18) does not hold at finite temperature, as the medium (i.e. the plasma) comprises a proper Lorentz frame and thus introduces a dependence of the self-energy on its local four-velocity u (cf. §4.1).

2.4 Modified Dirac's equation

As was shown previously, one of the useful aspects of the propagator is the fact that its poles yield the field's spectrum, i.e. the solutions of the Dirac equation that describes the field's motion (cf. (2.11), (2.12)). That means that the free propagator is the *inverse* of the Dirac operator that appears in Dirac's equation (2.6):

$$(\not{p} \mp m)S^0(p) \;=\; 1 \tag{2.19}$$

In fact, this is the definition of the propagator: it is the Green's function[2], in this case of the Dirac equation (i.e. it is the impulse solution of the equation of motion, 'impulse' meaning the RHS contains a delta function).

As for the dressed propagator, in the last section we showed it to have the form

[2] We are using the terms *Green's function* and *propagator* fairly interchangeably, but technically iS would be the propagator as used in field theoretical calculations, S being the Green's function of a differential equation.

$$
\begin{aligned}
S(p) &= \frac{1}{\not{p} - m - \Sigma(p) + i\epsilon} \\
&= \frac{1}{(1-A)\not{p} - (1+B)m + i\epsilon}.
\end{aligned} \tag{2.20}
$$

We then see that the self-energy changes the energy and the effective mass of the electron. However, we *know* the observed mass of a free electron, and thus this result needs reinterpretation. This requires a *regularisation* procedure and *renormalisation* of the self-energy. Renormalisation assures that the effective mass of the electron remains at its measured value in the dressed propagator, and at the same time makes the renormalised self-energy yield a finite, physical result [6].

The self-energy presented above is the basic phenomenon underlying the present work. However, we will be interested in its effect upon an electron that propagates inside a physical medium, rather than in a vacuum. To that end, we must include the *thermal* electron propagator in the calculation of the self-energy, instead of S^0 (2.11). Thermal propagators will be introduced in the next chapter. Essentially, rather than describing the propagation of a virtual electron (which may have *any* value of energy and will provoke the divergence of the self-energy), a thermal propagator represents the real electrons in the medium; therefore, the loop integration will be performed over a finite interval, limited by the energy distribution of the particles of the plasma. This will prevent its divergence, and thus regularisation will not be necessary.

Chapter 3

Finite temperature formalism

3.1 From vacuum to matter

In this work, we will be concerned with a description of a propagating e electron that accounts for the effects of a surrounding physical medium in thermodynamic equilibrium. Besides the coordinates available for the description of the electron in a vacuum, such as position, momentum, spin, etc., we now dispose of a set of thermodynamic state variables of the medium, such as inverse temperature β, volume V, chemical potential μ, particle density n, etc. As we know, to make the connection between quantum properties of microscopic systems, such as electrons, and the thermodynamics of a medium of macroscopic dimensions one must resource to quantum statistical physics. The objective of this chapter is to explain the transition from a 'zero temperature' field theory to one capable of accounting for the thermodynamics of the surrounding medium, that is to say a quantum field theory *at finite temperature and/or density.*

3.2 The classical density function

In the present work, as well as in the papers by Weldon [7, 8] reviewed in Chap. 4, the medium will always consist of a plasma of fermions (or of fermions and anti-fermions) in thermodynamic equilibrium. On the one hand, *thermal* equilibrium implies we can define one same value of temperature throughout the plasma that is also constant in time. Moreover, *chemical* equilibrium implies that the different species of particles in the medium that may react with each other, must not change their concentrations over time. Generally, one considers a chemical potential μ_i for each species i. Then, chemical equilibrium translates itself into equal values of μ_i for all interacting species in the plasma. In our study we will only consider interactions among one fermionic species, namely electrons and positrons, so we will only need one potential μ. Thus, an excess of electrons over positrons in the medium will give rise to a value of $\mu > 0$ (by convention), while an excess of positrons will yield $\mu < 0$. References [7, 8], for instance, which will be discussed in Chap. 4, focus on neuter plasmas, i.e. containing the same amount of fermions and antifermions of the same species, and thus consider $\mu = 0$. The work we have developed, on the other hand, concerns a totally degenerate electron gas, and the chemical potential will then be simply the Fermi energy, $\mu \equiv E_F$.

In statistical physics one wishes to calculate the statistical average of dynamic variables of a system, say, an electron. To that end, one creates an ensemble of a great number of replicas of that system. By *replicas* we mean systems described by the same Hamiltonian, which may however be in any given state at the moment of their creation[1]. The statistical averaging of a variable is then performed over all the systems of the ensemble. In general, there will be values of the dynamic variable that occur more often than others within the ensemble, and these will possess greter statistical weight.

In the classical theory, we describe the dynamic state of an element of the ensemble as a continuous function $\psi(\xi_i)$ of its general dynamic variables ξ_i, so that the state of each element of the ensemble corresponds to a point in phase space [20]. In the limit of an infinite number of elements in the ensemble (and therefore a continuum of points in phase space), we can divide phase space into infinitesimal portions $[\xi_i, \xi_i + \delta\xi_i]$, which we may *still* consider to contain a great amount of points. Then, it makes sense to define a density function $\rho(\xi_i)$ which gives the *fraction of systems* whose state is within the infinitesimal phase-space volume around ξ_i. But since the number of systems is infinite and they are all identical, such fraction equals the *probability* that any one random system of the ensemble is to be found in a state within $\psi[\xi_i, \xi_i + \delta\xi_i]$. In that sense, $\rho(\xi_i)$ is a *probability density function.*

As mentioned before, the thermal baths under study will consist of equal, independent particles. In that sense, we may perform statistically valid experiments by using the physical thermal bath as a realisation of a statistical ensemble. Classical statistical physics provides expressions for the density function ρ in terms of the thermodynamic variables of the ensemble. In paricular, because we will be interested in the study of baths with a definite value of inverse temperature β, chemical potential μ and volume V, we will use the density function of the so-called *grand canonical ensemble* [21]:

$$\rho(\beta, \mu, V, \xi_i) = Z^{-1} e^{-\beta(H - \mu N)}, \tag{3.1}$$

[1] As put by Gibbs [19], 'a great number of independent systems, identical in nature but independent in phase'.

where the denominator Z assures the condition

$$\int\limits_{\text{all ph. space}} d\xi_i \; \rho(\xi_i) = 1. \tag{3.2}$$

Thus, Z corresponds to the partition function of the ensemble,

$$Z = \int\limits_{\text{all ph. space}} d\xi_i \; e^{-\beta(H-\mu N)}, \tag{3.3}$$

where the Hamiltonian of the bath, H, is a function of the coordinates ξ_i, and N is the total number of particles in the system.

Now that we know an explicit form for the probability density function of the thermodynamic ensemble, the problem of finding the average of a given observable $O(\xi_i)$ of an individual element is reduced to calculating the integral

$$\langle O \rangle = \int\limits_{\text{all ph. space}} d\xi_i \; O(\xi_i) \; \rho(\xi_i). \tag{3.4}$$

3.3 Quantum statistics: the probability density operator

In quantum theory we cannot implement an expression for the probability density directly in phase space, as is the case of eq. (3.1), because in general the coordinates ξ_i do not commute [21]. If, however, we consider the state of each individual system to be described by a state vector in Hilbert space, $\big|\psi(\xi_i)\big\rangle$, we may hope to construct a probability density operator, $\hat{\rho}$, which would act upon any given state $\big|\psi(\xi_i)\big\rangle$ and yield the probability that a system of the ensemble be found in that state.

If our operator is to reflect the thermodynamics of the thermal bath, it must be an explicit function of a set of state variables describing the equilibrium state of the bath, $\hat{\rho} = \hat{\rho}\,(\beta,\, \mu,\, V)$, like the classical density function (3.1). Moreover, since we demand the bath to be in thermodynamic equilibrium, $\hat{\rho}$ must obviously be time-independent [21], so that the outcome of an observation of a particle of the bath will have the same probability regardless of when it is performed. This means the operator must *commute* with the Hamiltonian of the system,

$$[\hat{\rho}, \hat{H}] = 0, \tag{3.5}$$

as well as with any other conserved operators of the system. In other words, $\hat{\rho}$ must be a function of such conserved operators.

With all this in view, and in agreement with the classical prescription (3.1), one is driven to the form[2]

$$\hat{\rho}_\beta \propto e^{-\beta(\hat{H}-\mu\hat{Q})}, \tag{3.6}$$

where

$$\hat{Q} = \int_V d^3r\psi^\dagger\gamma^0\psi \tag{3.7}$$

is the field-operator form of the total fermionic charge contained in the thermal bath. The total number of particles N appearing in (3.1) has been replaced with the charge because the form of the QED Hamiltonian [6] implies that $\hat{Q}$ is a conserved operator, $[\hat{Q}, \hat{H}] = 0$, unlike in a classical system, where it is the total number of particles N that is conserved. From a particle point of view, Q is the total number of electrons minus the total number of positrons in a bath of volume V. On the contrary, in a quantum field theory such as QED the total number of particles in an isolated system is obviously not conserved, which is evident from phenomena such as electron-positron annihilation or pair production.

The form of $\hat{\rho}_\beta$ (3.6) implies that it shares all of its eigenstates with $\hat{H}$ as well as with $\hat{Q}$. Let $|\psi_i\rangle$ be a complete, orthonormal set of such eigenstates. We then have

$$\begin{aligned}\left\langle\psi_i\,\middle|\,\hat{\rho}_\beta\,\middle|\,\psi_j\right\rangle =&\rho_{ij}\left\langle\psi_i\,\middle|\,\psi_j\right\rangle\delta_{ij}\\ =&\rho_i\left\langle\psi_i\,\middle|\,\psi_i\right\rangle\\ =&e^{-\beta(H_i-\mu Q_i)}\left\langle\psi_i\,\middle|\,\psi_i\right\rangle.\end{aligned} \tag{3.8}$$

This is a diagonal matrix and each of its eigenvalues is proportional to the density function for the state $|\psi_i\rangle$. In order to interpret each eigenvalue as an actual probability we simply need to normalise the previous expression:

[2]The index β in eq. (3.6) is simply shorthand notation and serves as a reminder that the density operator contains the thermodynamic information regarding the bath. In fact, besides β, this form of the density operator is also an explicit function of μ, and depends implicitly on the volume V of the system through $\hat{H}$ and $\hat{Q}$.

$$\frac{\langle \psi_i \mid \hat{\rho}_\beta \mid \psi_i \rangle}{\sum_i \langle \psi_i \mid \hat{\rho}_\beta \mid \psi_i \rangle} = \frac{\langle \psi_i \mid \hat{\rho}_\beta \mid \psi_i \rangle}{\mathrm{tr} \langle \psi_i \mid \hat{\rho}_\beta \mid \psi_i \rangle} = Z_\beta^{-1} \langle \psi_i \mid \hat{\rho}_\beta \mid \psi_i \rangle , \tag{3.9}$$

where Z_β is the partition function of the thermal bath, which is now written as the trace of a matrix in Hilbert space. Being a trace, its value does not depend on the particular choice of complete vector basis, which allows us to relax the condition that $|\psi_i\rangle$ be energy eigenstates. Thus, in general, one may write the normalised probability density operator (3.9) using the somewhat lighter notation:

$$Z_\beta^{-1} \hat{\rho}_\beta = \frac{1}{\mathrm{tr}\, \hat{\rho}_\beta} \hat{\rho}_\beta. \tag{3.10}$$

Thus, to obtain the probability of any general state, $\hat{\rho}_\beta$ is to be placed between a bra and a ket of that state, as written explicitly in eq. (3.9), and tr $\hat{\rho}_\beta$, after being calculated using *any* complete basis, becomes just a c-number.

3.4 Thermal quantum operators

The statistical postulate of quantum mechanics [22] states that if we measure a great number of times the value of an observable $\hat{O}$ of a system in a given state $|\psi_i\rangle$, we can write the average of the measurements as the expectation value of $\hat{O}$ in that state,

$$\langle O \rangle_i = \left\langle \psi_i \middle| \hat{O} \middle| \psi_i \right\rangle . \tag{3.11}$$

If, on the other hand, we now consider a statistical ensemble, the question is what will be the average outcome of measuring observable $\hat{O}$ *in a great number of random elements of the ensemble.* Using the arguments of the previous section, one finds

$$\begin{aligned} \langle O \rangle_\beta =& Z_\beta^{-1} \sum_i \left\langle \psi_i \middle| \hat{\rho}_\beta \hat{O} \middle| \psi_i \right\rangle \\ =& \frac{\sum_i \left\langle \psi_i \middle| \hat{\rho}_\beta \hat{O} \middle| \psi_i \right\rangle}{\sum_i \langle \psi_i \mid \hat{\rho}_\beta \mid \psi_i \rangle} \end{aligned}$$

$$= \frac{\text{tr}\{\hat{\rho}_\beta \hat{O}\}}{\text{tr}\,\hat{\rho}_\beta} \tag{3.12}$$

where $|\psi_i\rangle$ is a complete set of states of the system which, again, need not be eigenstates of either $\hat{\rho}_\beta$ or $\hat{O}$, since both the numerator and the denominator are matrix traces and therefore invariant. Also, note that the order of the operators in the numerator is irrelevant, because of the so-called *cyclic property* of the trace:

$$\text{tr}\{\hat{O}_1\hat{O}_2...\hat{O}_N\} = \text{tr}\{\hat{O}_2...\hat{O}_N\hat{O}_1\}. \tag{3.13}$$

Equation (3.12) prescribes the form of the thermal average of an operator (or in more relaxed language, a 'thermal operator'), which is in the heart of finite temperature field theory, particularly the so-called *real-time formalism*, which will be the method used throughout this work.

3.5 The thermal propagator, S_β

As we have discussed in the previous chapter, the electron propagator in zero temperature QED is given in position space by

$$\begin{aligned} iS^{\alpha\beta}(x,x') &= \left\langle T\left[\psi^\alpha(x)\bar{\psi}^\beta(x')\right]\right\rangle \\ &= \left\langle 0 \middle| T\left[\psi^\alpha(x)\bar{\psi}^\beta(x')\right] \middle| 0 \right\rangle . \end{aligned} \tag{3.14}$$

As we have also discussed, the expressions ψ and $\bar{\psi}$ are operators in the interaction picture, so that in view of eq. (3.12) we can write the thermal average of the propagator as

$$\begin{aligned} iS_\beta(x,x') &= \left\langle T\left[\psi(x)\bar{\psi}(x')\right]\right\rangle_\beta \\ &= Z_\beta^{-1}\,\text{tr}\left\{\rho_\beta T\left[\psi(x)\bar{\psi}(x')\right]\right\} \\ &= Z_\beta^{-1}\,\text{tr}\left\{e^{-\beta(\hat{H}-\mu\hat{Q})} T\left[\psi(x)\bar{\psi}(x')\right]\right\}, \end{aligned} \tag{3.15}$$

where the spinor indices $\alpha\beta$ have been omitted for clarity of notation. For the same reason, let us make two other simplifications: first, define $\hat{H}_\mu = \hat{H} - \mu\hat{Q}$; secondly, let us note that because of thermal equilibrium and the homogeneity of the medium, S_β must not depend on the specific coordinates $x = (t, \mathbf{x})$, $x' = (t', \mathbf{x}')$, but only on their difference, $S_\beta(x, x') = S_\beta(x - x')$. This also allows us to choose the value $x' = 0$ without loss of generality and solely for ease of notation. The *thermal fermionic propagator* (3.15) may then be written in the simpler form

$$iS_\beta(x) = Z_\beta^{-1} \,\mathrm{tr}\left\{e^{-\beta\hat{H}_\mu} T\left[\psi(x)\bar{\psi}(0)\right]\right\}. \tag{3.16}$$

Comparing this expression with the zero temperature electron propagator (3.14), one realises that the presence of a thermal medium obliges to the averaging of the propagator over all possible states, rather than just the vacuum.

We will now derive the expression for the thermal electron propagator directly from its definition (3.16) – a path that to our knowledge has not been followed in the literature, and which we believe to be the most demystifying.

To that purpose, let us now work with a basis of energy eigenstates (which are also eigenstates of the total charge $\hat{Q}$). In particular, we may use the basis $|n\rangle$, given by the states consisting of n particles of the field, all bearing the same definite momentum $\mathbf{p}$. Because we are dealing with a fermionic field, this basis has only two non-vanishing states, $|0\rangle$ and $|1\rangle$, because of Pauli's exclusion principle. Therefore, the trace in eq. (3.16) consists simply of a two-term sum:

$$iS_\beta(x) = \frac{\left\langle 0 \left| e^{-\beta\hat{H}_\mu} T\left[\psi(x)\bar{\psi}(0)\right] \right| 0 \right\rangle + \left\langle 1 \left| e^{-\beta\hat{H}_\mu} T\left[\psi(x)\bar{\psi}(0)\right] \right| 1 \right\rangle}{\left\langle 0 \left| e^{-\beta\hat{H}_\mu} \right| 0 \right\rangle + \left\langle 1 \left| e^{-\beta\hat{H}_\mu} \right| 1 \right\rangle} \tag{3.17}$$

Because these states are eigenstates of $\hat{H}_\mu$, the density operator $e^{-\beta\hat{H}_\mu}$ will simply yield a c-number factor for each bracket. Let us suppose

$$H_\mu^{(0)} = H^{(0)} - \mu\, Q^{(0)} \tag{3.18}$$

to be the eigenvalue of $\hat{H}_\mu$ corresponding to the ground state of the system, $|0\rangle$. Then, regardless of the actual values of $H^{(0)}$ and $Q^{(0)}$, we know the energy of state $|1\rangle$ will be

$$
\begin{aligned}
H_\mu^{(1)} =& (H^{(0)} + E_p) - \mu \, (Q^{(0)} \pm 1) \\
=& H_\mu^{(0)} + E_p \mp \mu.
\end{aligned}
\tag{3.19}
$$

The charge $(Q^{(0)} \,{}^{+}_{(-)} 1)$ corresponds to the particle in state $|1\rangle$ being an electron (positron), since each carries one positive (negative) unit of charge, as conventionalised by the definition of $\hat{Q}$ (3.7). We may then rewrite (3.17) as

$$
\begin{aligned}
iS_\beta(x) =& \frac{e^{-\beta H_\mu^{(0)}} \left\langle 0 \middle| T\left[\psi(x)\bar{\psi}(0)\right] \middle| 0 \right\rangle + e^{-\beta(H_\mu^{(0)} + E_p \mp \mu)} \left\langle 1 \middle| T\left[\psi(x)\bar{\psi}(0)\right] \middle| 1 \right\rangle}{e^{-\beta H_\mu^{(0)}} \langle 0 \,|\, 0 \rangle + e^{-\beta(H_\mu^{(0)} + E_p \mp \mu)} \langle 1 \,|\, 1 \rangle} \\
=& \frac{\left\langle 0 \middle| T\left[\psi(x)\bar{\psi}(0)\right] \middle| 0 \right\rangle + e^{-\beta(E_p \mp \mu)} \left\langle 1 \middle| T\left[\psi(x)\bar{\psi}(0)\right] \middle| 1 \right\rangle}{\langle 0 \,|\, 0 \rangle + e^{-\beta(E_p \mp \mu)} \langle 1 \,|\, 1 \rangle} \\
=& \frac{\left\langle 0 \middle| T\left[\psi(x)\bar{\psi}(0)\right] \middle| 0 \right\rangle + e^{-\beta(E_p \mp \mu)} \left\langle 1 \middle| T\left[\psi(x)\bar{\psi}(0)\right] \middle| 1 \right\rangle}{1 + e^{-\beta(E_p \mp \mu)}} \\
=& \frac{e^{\beta(E_p \mp \mu)}}{1 + e^{\beta(E_p \mp \mu)}} \left\langle 0 \middle| T\left[\psi(x)\bar{\psi}(0)\right] \middle| 0 \right\rangle + \frac{1}{1 + e^{\beta(E_p \mp \mu)}} \left\langle 1 \middle| T\left[\psi(x)\bar{\psi}(0)\right] \middle| 1 \right\rangle \\
=& \left(1 - \frac{1}{1 + e^{\beta(E_p \mp \mu)}}\right) \left\langle 0 \middle| T\left[\psi(x)\bar{\psi}(0)\right] \middle| 0 \right\rangle + \frac{1}{1 + e^{\beta(E_p \mp \mu)}} \left\langle 1 \middle| T\left[\psi(x)\bar{\psi}(0)\right] \middle| 1 \right\rangle \\
=& (1 - n_F) \left\langle 0 \middle| T\left[\psi(x)\bar{\psi}(0)\right] \middle| 0 \right\rangle + n_F \left\langle 1 \middle| T\left[\psi(x)\bar{\psi}(0)\right] \middle| 1 \right\rangle.
\end{aligned}
\tag{3.20}
$$

Note the natural emergence of the Fermi-Dirac distribution function,

$$
n_F(\beta, \mu, p) = \frac{1}{1 + e^{\beta(E_p \mp \mu)}}, \tag{3.21}
$$

where, again, the $\mp$ sign refers to electrons and positrons respectively. We may easily separate the zero- and finite-temperature terms in (3.20):

$$
\begin{aligned}
iS_\beta(x) =& iS(x) - n_F\Big(\Big\langle 0 \Big| T\left[\psi(x)\bar{\psi}(0)\right] \Big| 0 \Big\rangle - \Big\langle 1 \Big| T\left[\psi(x)\bar{\psi}(0)\right] \Big| 1 \Big\rangle \Big) \\
=& iS(x) + iS'_\beta(x),
\end{aligned} \tag{3.22}
$$

Henceforth, our concern will be the calculation of the temperature-dependent term $S'_\beta(x)$, since we have already dealt with the zero temperature term in the previous chapter (cf. (2.11)).

The free thermal propagator

As we have seen, the free particle-field operators $\psi(x)$, $\bar{\psi}(x)$ have the following representation in position space:

$$
\begin{aligned}
\psi(x) =& \sum_s \int \frac{d^3p}{(2\pi)^3 2E_p} \left(b_s(p) u_s(p) e^{-ip\cdot x} + d_s^\dagger(p) v_s(p) e^{ip\cdot x} \right) \\
\bar{\psi}(x) =& \sum_s \int \frac{d^3p}{(2\pi)^3 2E_p} \left(b_s^\dagger(p) \bar{u}_s(p) e^{-ip\cdot x} + d_s(p) \bar{v}_s(p) e^{ip\cdot x} \right)
\end{aligned} \tag{3.23}
$$

where $p \cdot x \equiv E_p t - \mathbf{p} \cdot \mathbf{x}$.

Substitution of the expressions (3.23) in (3.20) shows that the product $T(\psi\bar{\psi})$ yields several pairs of operators, each pair ordered in a specific way and attached to a theta function $\theta(\pm t)$, which proceeds from the time ordering. At zero temperature, because the propagator (3.14) is evaluated in the ground state, we saw that all terms vanished except the ones containing the operator structure $b_s b_s^\dagger$ and $d_s d_s^\dagger$ (placed in that order). In S'_β (3.22), however, there is now a second term where the product is evaluated in the state $|1\rangle$, so that the combinations containing $d_s^\dagger d_s$ and $b_s^\dagger b_s$ will be the ones to survive. Inserting (3.23) into S'_β in (3.22) then yields (omitting the (p) dependence of the operators and spinors)

$$iS'_\beta(x) = -n_F \sum_s \int \frac{d^3p}{(2\pi)^3 2E_p} \Bigg\{ \Big\langle 0 \Big| \theta(t) b_s b_s^\dagger u_s \bar{u}_s e^{-ip\cdot x} - \theta(-t) d_s d_s^\dagger \bar{v}_s v_s e^{ip\cdot x} \Big| 0 \Big\rangle$$
$$- \Big\langle 1 \Big| \theta(t) d_s^\dagger d_s v_s \bar{v}_s e^{ip\cdot x} - \theta(-t) b_s^\dagger b_s \bar{u}_s u_s e^{-ip\cdot x} \Big| 1 \Big\rangle \Bigg\}. \tag{3.24}$$

Trivially applying the operators to the states, and performing the sum over spins $s = \pm 1/2$ according to the known result [6]

$$\sum_s u_s \bar{u}_s = \not{p} + m$$
$$\sum_s v_s \bar{v}_s = \not{p} - m, \tag{3.25}$$

we obtain straightforwardly

$$\begin{aligned} iS'_\beta(x) =& - n_F \int \frac{d^3p}{(2\pi)^3 2E_p} \Big[\theta(t)(\not{p} + m) e^{-ip\cdot x} - \theta(-t)(\not{p} - m) e^{ip\cdot x} \\ & - \theta(t)(\not{p} - m) e^{ip\cdot x} + \theta(-t)(\not{p} + m) e^{-ip\cdot x} \Big] \\ =& - n_F \int \frac{d^3p}{(2\pi)^3 2E_p} \Big[(\not{p} + m) e^{-ip\cdot x} - (\not{p} - m) e^{ip\cdot x} \Big]. \end{aligned} \tag{3.26}$$

We recall that until this point the time component p_0 has been considered fixed at $p_0 = E_p = \sqrt{\mathbf{p}^2 + m^2}$, so that $\not{p} = E_p \gamma_0 - \mathbf{p} \cdot \vec{\gamma}$ and $p \cdot x = E_p t - \mathbf{p} \cdot \mathbf{x}$. Let us now instead write out the time integral explicitly, containing the energy Dirac delta:

$$\begin{aligned} iS'_\beta(x) =& - n_F \int \frac{d^4p}{(2\pi)^4 2E_p} \Big[(p_0 \gamma_0 - \mathbf{p} \cdot \vec{\gamma} + m) e^{-i(p_0 t - \mathbf{p}\cdot\mathbf{x})} \\ & + (-p_0 \gamma_0 + \mathbf{p} \cdot \vec{\gamma} + m) e^{i(p_0 t - \mathbf{p}\cdot\mathbf{x})} \Big] 2\pi \delta(p_o - E_p). \end{aligned}$$

Making $\mathbf{p} \to -\mathbf{p}$ in the second term yields:

$$= -\, n_F \int \frac{d^4p}{(2\pi)^4 2E_p} e^{i\mathbf{p}\cdot\mathbf{x}} \Big[(p_0\gamma_0 - \mathbf{p}\cdot\vec{\gamma} + m) e^{-ip_0 t} + (-p_0\gamma_0 - \mathbf{p}\cdot\vec{\gamma} + m) e^{ip_0 t} \Big]$$

$$\times\, 2\pi\delta(p_o - E_p)$$

$$= -\, n_F \int \frac{d^4p}{(2\pi)^4 2E_p} e^{-i(p_0 t - \mathbf{p}\cdot\mathbf{x})} (p_0\gamma_0 - \mathbf{p}\cdot\vec{\gamma} + m) \times 2\pi \Big[\delta(p_0 - E_p) + \delta(p_0 + E_p) \Big]$$

$$= -\, n_F \int \frac{d^4p}{(2\pi)^4} e^{-ip\cdot x} (\not{p} + m) 2\pi\delta(p_0^2 - E_p^2) \tag{3.27}$$

The latter integral has the exact form of a Fourier transform; therefore, the integral kernel corresponds to the expression for S_β in momentum space:

$$S'_\beta(p) = n_F (\not{p} + m) 2\pi i \delta(p_0^2 - E_p^2) \tag{3.28}$$

(we have multiplied both sides by $-i$). Recalling the expression derived in the previous chapter for the zero temperature free field propagator in momentum space, eq. (2.11), and adding it to result (3.28), we obtain the full momentum-space representation of the thermal averaged free propagator,

$$S_\beta(p) = (\not{p} + m) \left(\frac{1}{p^2 - m^2 + i\epsilon} + n_F 2\pi i \delta(p_0^2 - E_p^2) \right) \tag{3.29}$$

We notice that the propagator is separated into a temperature-independent term, identical to the Feynman propagator in a vacuum (2.11), and a second term that contains all the information regarding the physical medium; such information lies solely in the Fermi-Dirac distribution function, $n_F(\beta, \mu)$.

Equally important is the fact that the temperature-dependent term describes an on-shell contribution, because of the Dirac delta. This exposes the meaning of the thermal propagator: when considering the presence of a medium, we must add to the (causal) propagator describing our virtual particle a second term describing the simultaneous propagation of the particles of the medium, which are real and therefore lie on the mass shell, and whose distribution in momentum space is given by n_F.

For completeness, we will add that the free photon propagator in thermal QED is given by an equivalent expression, namely [5]

$$D_{\beta}^{\mu\nu}(k) = -ig^{\mu\nu}\left(\frac{1}{k^2 + i\epsilon} - n_B 2\pi i\delta(k^2)\right) \tag{3.30}$$

Here, $n_B = (1 - e^{\beta H})^{-1}$ the Bose-Einstein distribution function. In this work, photon density will be considered low, and thus the thermal corrections to the photon propagator will not be studied.

By replacing the zero-temperature free Feynman propagator S^0 (2.11) with the thermal propagator (3.29), in Chap. 5 In the next chapter we will first explore this method, giving as example some of the literature on ths topic [7] where the same formalism was applied to a symmetric plasma of massless electrons and positrons in the high-temperature regime.

Chapter 4

Calculation of the thermal self-energy to one-loop order

This chapter introduces the thermal self-energy calculations and reviews some of the results published in the past, as an example of application. Namely, we will focus on some of the work by H. A. Weldon [7–9] regarding hot symmetric plasmas of massless fermions. Thus, the whole chapter will focus on the particular case of massless fermions (in our case, electrons). The consideration of a finite electron mass will be left for Chap. 5 where we will study a cold plasma of massive electrons with very high chemical potential.

We will start by introducing in §4.1 the calculation of the self-energy at finite temperature using the thermal propagator (3.28) applied to massless electrons. In §4.2 we will discuss the physical meaning of the formalism. In §4.4 Weldon's procedure will be adapted and the results will be presented as an example of application of the formalism. Finally, in §4.5 we will explain theoretically how the hole excitations arise as solutions of the Dirac equation in a thermal medium and describe some of the properties of these excitations.

4.1 Structure of the thermal self-energy

Throughout this chapter we will consider as thermomdynamic medium a symmetric plasma in the very high-temperature regime. 'Symmetric' in this context means that it contains electrons and positrons with equal energy distributions. This yields zero chemical potential, so that the Fermi-Dirac distribution function (3.21) simplifies to

$$n_F(\beta, p) = \frac{1}{1 + e^{\beta E_p}}. \tag{4.1}$$

Furthermore, we will suppose the system to be chirally invariant, which means that the electrons and positrons of the plasma will be considered massless. The study of systems of massless fermions is particularly relevant at very high temperatures where chiral symmetry is restored, as shown by Weinberg [23].

The self-energy to one-loop order may then be written, in parallel with the zero-temperature case (2.15):

$$\begin{aligned}\Sigma =& e^2 \int \frac{d^4p'}{(2\pi)^4} D^0_{\mu\nu}(p - p')\gamma^\mu S_\beta(p')\gamma^\nu \\ =& - ie^2 \int \frac{1}{(p - p')^2 + i\epsilon} \gamma^\mu \not{p}' \gamma_\mu \left(\frac{1}{p'^2 + i\epsilon} + in_F(p') 2\pi\delta(p'^2) \right).\end{aligned} \tag{4.2}$$

We notice immediately that because of the separability of the propagator into a zero-temperature and a finite-temperature term, the one-loop self-energy may also be separated in that manner:

$$\begin{aligned}\Sigma =& - ie^2 \int \frac{d^4p'}{(2\pi)^4} \gamma^\mu \not{p}' \gamma_\mu \left(\frac{1}{[(p - p')^2 + i\epsilon][p'^2 + i\epsilon]} + 2\pi i \frac{n_F(p')\delta(p'^2)}{(p - p')^2 + i\epsilon} \right) \\ =& \Sigma^{(T=0)} + \Sigma_\beta.\end{aligned} \tag{4.3}$$

The first term is just the zero-tempearture self-energy (2.15); as discussed in §2.4, by means of regularisation of the integral followed by renormalisation of the constants one can make this self-energy yield the normal value of mass and energy of a free electron, so our only concern henceforth will be the temperature-dependent term Σ_β (for simplicity, we will call this term the *thermal self-energy*):

$$\Sigma_\beta = -e^2 \int \frac{d^4p'}{4\pi^3} \frac{\not{p}'}{(p - p')^2 + i\epsilon} n_F(p')\delta(p'^2), \tag{4.4}$$

where the gamma matrices in (4.3) have been resolved using the identity $\gamma^\mu \not{p}' \gamma_\mu = -2\not{p}'$.

We discussed in Chap. 2 how the self-energy of an electron in a vacuum may only depend on the electron's energy and momentum. However, in a physical medium there is an additional Lorentz frame to be taken into account, namely the rest frame of the fluid. This frame is defined by a four-velocity $u = (1, \mathbf{v})$, which is the local velocity of the particles of the plasma. With this definition, we may rewrite the particle distribution function n_F in the following covariant form [7]:

$$n_F(p', u) = \frac{1}{1 + e^{\beta|p' \cdot u|}}, \tag{4.5}$$

Notice that in the earlier definition of the distribution function we had made use of the particle's energy $E_{p'}$ in its own rest frame. With this new definition we generalise the formalism to any rest frame, by working with the Lorentz invariant $p' \cdot u$. At the same time, we are introducing in the thermal propagator a formal dependence on the fluid's velocity u^μ, which is a conceptually fundamental aspect of the theory. Notice that in the plasma's own rest frame we have $u = (1, 0, 0, 0)$, and the distribution function falls back into its earlier definition (3.21).

Because of the inclusion in the theory of the rest frame of the plasma, the structure of the self-energy of an electron no longer depends solely on its momentum, as was the case in a vacuum (cf. eq. (2.18)). Rather, we must now write

$$\Sigma(p, u) = -a\not{p} - b\not{u}, \tag{4.6}$$

where the minus signs are purely conventional. Note there is no term proportional to the unit matrix as in (2.18) because we are considering zero electron mass – this aspect will change for the system studied in the next chapter.

This form of Σ will confer the dressed thermal propagator a different structure than that at zero temperature:

$$S_\beta(p, u) \;=\; \frac{1}{\not{p} - \Sigma(p, u) + i\epsilon} \;=\; \frac{1}{(1 + a)\not{p} + b\not{u} + i\epsilon}. \tag{4.7}$$

In §4.4 we will see how this propagator may be used to obtain the excitation spectrum

However, before we perform such calculation we would like to make some conceptual considerations on the physical meaning of the finite-temperature self-energy diagram, in terms of the processes among the particles of the plasma.

4.2 Physical meaning of the thermal self-energy

The one-loop thermal self-energy diagram may be represented as shown in fig. 4.1.

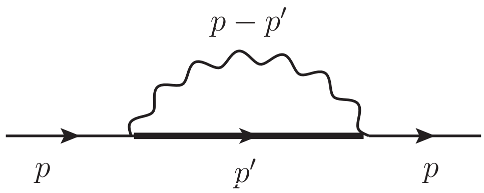

FIGURE 4.1: Diagram of the thermal electron self-energy. A bold line is used in the present work to represent the thermal electron propagator, which represents a real electron of the thermal bath.

We have used a bold line to represent the fact that the corresponding propagator is to be calculated at finite temperature, i.e. taking into account the particle distribution in the physical medium, namely (as was discussed in Chap. 3),

$$S_\beta(p') = (\not{p}' + m)\left(\frac{1}{p'^2 - m^2 + i\epsilon} + n_F(p')2\pi i\delta(p_0'^2 - E_{p'}^2)\right) \tag{4.8}$$

The part of the self-energy loop that is strictly temperature-dependent, which we have called Σ_β, involves only the second term in (4.8). This term accounts for the propagation of real particles (note that the delta function places them on their mass shell) with an energy distribution characterised by $n_F(p')$. Therefore, by calculating the temperature-dependent term of the self-energy loop of fig. 4.1, we are in fact calculating the amplitude of a scattering-like process between our propagating electron and a real electron or positron of the medium, summed over all values of momentum p' available from the distribution function. This scattering is represented in fig. 4.2(a) for the case where the particle of the bath is an electron, and fig. 4.2(b) for the case of a positron.

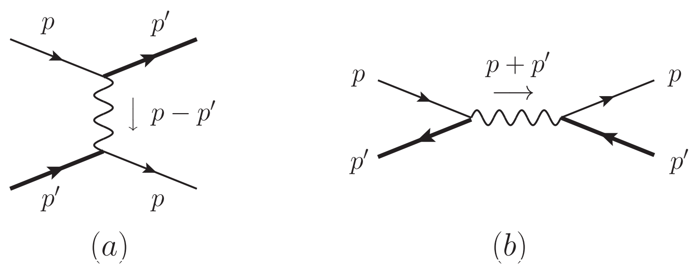

FIGURE 4.2: Diagrams representing (a) the exchange interaction between a thermalised electron and an electron of the thermal bath (b) a similar scatterig process with exchange of momenta between a thermalised electron and a positron of the thermal bath.

On the other hand, consider the tadpole diagram of fig. 2.1(b). This will correspond to the t-channel diagram of fig. 4.3(a) representing the forward scattering between the propagating electron and an electron of the thermal bath, represented in bold. In diagram 4.2(b) we consider the case where a positron of the medium participates in the interacion.

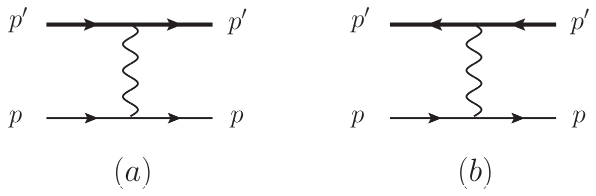

FIGURE 4.3: Diagrams representing the direct interaction, where a thermalised electron forward scatters off an (a) electron (b) positron of the thermal bath.

Now suppose that the thermal medium is neuter as a whole, which is usually the case for most physical systems of interest. Then, when we perform the integral of the tadpole diagram over the 4-momentum p', because there is no momentum exchange between the interacting particles, each infinitesimal contribution from dp'_0 and $-dp'_0$, arising from either diagram in fig. 4.3 will cancel, and the result will be zero. We have hence justified our statement made in §2.1 that the tadpole diagram may be ignored in the context of this work.

On the contrary, when considering the diagrams representative of the self-energy, fig. 4.2, we see that the propagating particle will have a different interaction with a plasma particle with energy-momentum $(p'_0, \mathbf{p}')$ than with one having energy-momentum $(-p'_0, \mathbf{p}')$, since in one case the process will occur via s-channel, with the exchanged photon having the sum of the particle's momenta (fig. 4.2(a)), and in the other case via t-channel, with the photon carrying the difference of the momenta (fig. 4.2(b)). Thus, an integration over all values of $p'_0, \mathbf{p}'$ will not cancel through.

In the case of a degenerate electron plasma, which will be treated in the next chapter, there exist no positrons in the medium that could cancel the tadpole contribution; however, if we consider a neuter plasma there will be a different species of positively charged fermions, such as protons, that will interact electromagnetically with a propagating electron as in fig. 4.3(b), and thus cancel the overall contribution of the tadpole.

4.3 On the imaginary self-energy

The photon propagator (4.9) has simple poles at $(p_0 - p'_0)^2 = (\mathbf{p} - \mathbf{p}')^2 - i\epsilon$. A simple-poled analytic function bay be decomposed as [24]

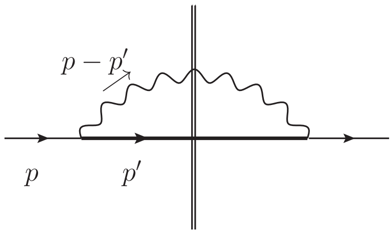

FIGURE 4.4: Contribution to the imaginary component of the self-energy at one loop: a thermalised electron with a given invariant mass $p_0^2 - \mathbf{p}^2 \neq m^2$ decays into a real electron and a real photon.

$$iD_0(p - p') = \frac{1}{(p - p')^2 + i\epsilon} = \mathcal{P}\left\{\frac{1}{(p - p')^2}\right\} - i\pi\delta[(p - p')^2], \tag{4.9}$$

where we have omitted the metric $g_{\mu\nu}$ for simplicity, and $\mathcal{P}$ stands for the Cauchy principal value. In general, loop corrections may have an absorptive contribution from an imaginary part. This will correspond to the amplitude of both particles on the loop becoming real, which amounts to the decay of the propagating electron, as represented in fig. 4.4. In principle, one could hope to extract information on the lifetime of the thermalised electrons, and thus make conclusions on the stability of the plasma. However, the decay rate depends on kinematic constraints that can only be known once the dispersion relation of the electron is calculated and the energy spectrum of the system is known. Because we do not yet know the thermal correction to the electron mass, we will disregard the imaginary part of the self-energy and limit ourselves to the calculation of the real part:

The scope of the present work, namely the calculation of the self-energy to one-loop order, prevents us from extracting physical results from the imaginary part of the thermal self-energy. Rather, we will focus on its real part:

$$\mathrm{Re}\,\Sigma_\beta(p) = -e^2 \int \frac{d^4p'}{4\pi^3} \frac{\not{p}'}{(p - p')^2} n_F(p')\delta(p'^2). \tag{4.10}$$

For ease of notation, hereafter Σ_β will always denote the real part of the thermal self-energy, and S_β the real part of the thermal electron propagator.

4.4 Fermionic modes in a high-temperature plasma

As we have discussed in §2.4, the poles of the propagator yield the field's excitation spectrum. In order to calculate the poles of propagator (4.7) we must first resolve the spinorial structure of its denominator:

$$
\begin{aligned}
S_\beta(p,u) &= \frac{1}{(1+a)\not{p}+b\not{u}} \\
&= \frac{(1+a)\not{p}+b\not{u}}{(1+a)^2p^2+2(1+a)bp\cdot u+b^2}
\end{aligned} \tag{4.11}
$$

where we have used the fact that $u^2 = u^\mu u_\mu = 1$. Thus, the energy spectrum is now given by the (real-valued) solutions of the equation

$$
\begin{aligned}
\mathcal{F}^2(p_0,\mathbf{p}) = 0 \\
\Longrightarrow\ (1+a)^2p^2+2(1+a)b(p\cdot u)+b^2 = 0 \\
\Longrightarrow\ (1+a)^2(p_0^2-\mathbf{p}^2)+2(1+a)bp_0+b^2 = 0 \\
\Longrightarrow\ [(1+a)p_0+b]^2-(1+a)^2\mathbf{p}^2 = 0 \\
\Longrightarrow\ \big[(1+a)(p_0-|\mathbf{p}|)+b\big]\big[(1+a)(p_0+|\mathbf{p}|)+b\big] = 0 \\
\Longrightarrow\ \mathcal{F}_1(p_0,\mathbf{p})\mathcal{F}_2(p_0,\mathbf{p}) = 0
\end{aligned} \tag{4.12}
$$

Again, notice that because $p\cdot u$ is a Lorentz invariant we may calculate it in any frame of reference; we have chosen the rest frame of the physical medium, for which $u = (1,\vec{0})$. An expression of this kind, relating the energy of the propagating particle with its momentum, is called a *dispersion relation*. Knowledge of the dispersion relation would instruct us on the energy of a particle of a certain momentum $\mathbf{p}$ as it propagates through the medium and, as we can see, such knowledge amounts to the calculation of the parameters a and b, which themselves depend on p_0 and $|\mathbf{p}|$.

Using the gamma matrix trace identity [6] $\mathrm{tr}\,\not{a}\not{b} = 4a\cdot b$, we may extract a and b from definition (4.6):

$$
\frac{1}{4}\,\mathrm{tr}\left\{\not{p}\Sigma_\beta\right\} = -\,ap^2 - bp\cdot u = -ap^2 - bp_0 \tag{4.13a}
$$

$$
\frac{1}{4}\,\mathrm{tr}\left\{\not{u}\Sigma_\beta\right\} = -\,ap\cdot u - bu^2 = -ap_0 - b, \tag{4.13b}
$$

whence

$$a(p_0,|\mathbf{p}|) = \frac{1}{4p^2}\,\mathrm{tr}\{(\not{p} - p_0\not{u})\Sigma_\beta\}$$

$$= -\frac{1}{4p^2}\,\mathrm{tr}\{(\mathbf{p}\cdot\boldsymbol{\gamma})\Sigma_\beta\} \tag{4.14a}$$

$$(ap_0 + b)[p_0,|\mathbf{p}|] = -\frac{1}{4}\,\mathrm{tr}\{\not{u}\Sigma_\beta\}$$

$$= -\frac{1}{4}\,\mathrm{tr}\{\gamma_0\Sigma_\beta\}, \tag{4.14b}$$

where we have chosen to calculate these quantities in the rest frame of the plasma, $u = (1,\vec{0})$. From these expressions we can see that $ap_0 + b$ is the time component of Σ_β measured in the rest frame of the plasma and a is the projection of the spatial component of Σ_β on the momentum of the propagating particle.

We now understand that it is the dependence of the thermal self-energy on the plasma velocity u what ultimately spoils the Lorentz invariance of the dispersion relation, by making it depend separately on the individual components p_0 and $|\mathbf{p}|$. On the contrary, in a vacuum the dispersion relation depends only on $p^2 = p_0^2 - \mathbf{p}^2$.

In summary, one must calculate the self-energy loop Σ_β, extract the approximated values of the self-energy functions defined in (4.14) and thus obtain an expression for the dispersion relation (4.12), which will be of the form $\mathcal{F}_1(p_0,\mathbf{p})\mathcal{F}_2(p_0,\mathbf{p}) = 0$.

The calculation of the projections of the self-energy Σ_β has been adapted from reference [7] and is shown in detail in appendix C. For large values of temperature T, the following approximations are obtained:

$$(ap_0 + b)[p_0,|\mathbf{p}|] \approx (eT)^2\frac{1}{16|\mathbf{p}|}\log\frac{p_0 - |\mathbf{p}|}{p_0 + |\mathbf{p}|} \tag{4.15a}$$

$$a(p_0,|\mathbf{p}|) \approx \frac{e^2T^2}{8\mathbf{p}^2}\left[1 - \frac{p_0}{2|\mathbf{p}|}\log\frac{p_0 + |\mathbf{p}|}{p_0 - |\mathbf{p}|}\right] \tag{4.15b}$$

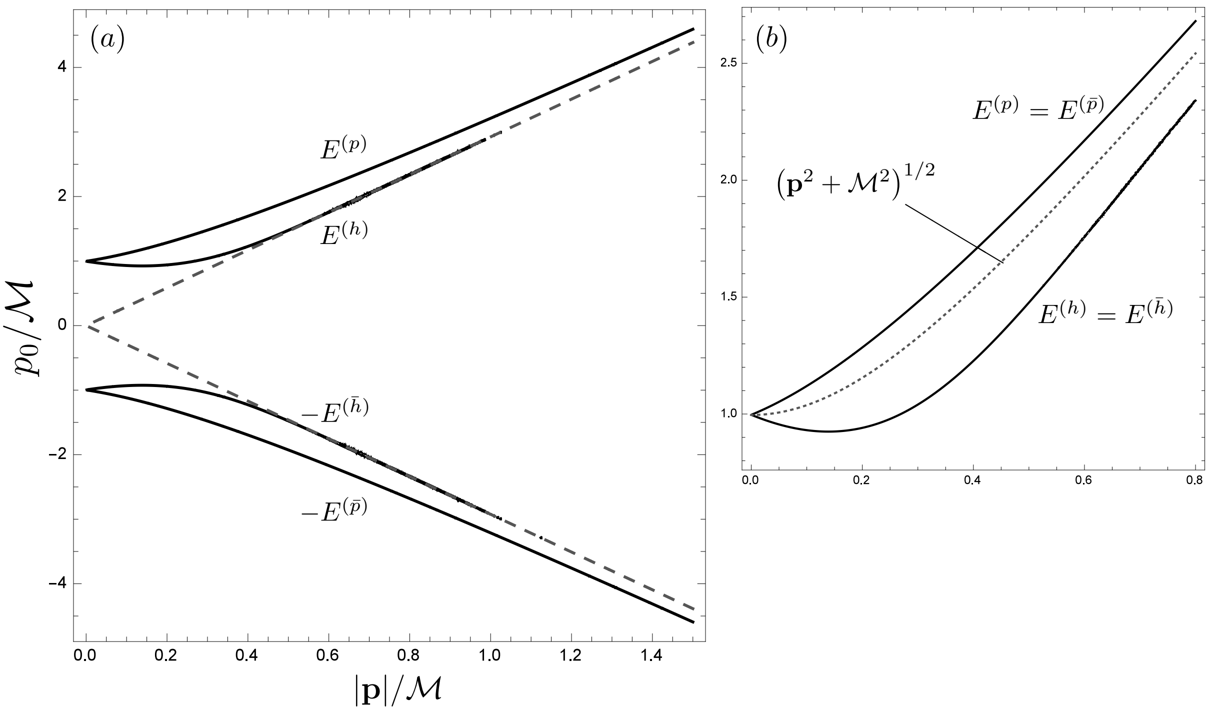

FIGURE 4.5: (a) Dispersion relations of the four chirally invariant fermionic modes of a high-temperature symmetric plasma. The dashed lines correspond to a free massless fermion, $p_0 = \pm|\mathbf{p}|$. (b) Close-up of the particle and hole modes. The dotted curve is the energy of a free fermion of mass $\mathcal{M}$, for comparison. These plots correspond to the numerical solutions of eq. (C.13).

These functions may now be substituted in the electron's dispersion relation, eq. (4.12). This result is presented in an implicit form in appendix C (eq. (C.13)). Furthermore, we have computed this equation numerically[1], and the resulting plot is shown in 4.5(a).

The plot shows the presence of four excitations, labelled $E^{(p)}$, $E^{(\bar{p})}$, $E^{(h)}$ and $E^{(\bar{h})}$, where the indices stand for *(anti)particle* and *(anti-)hole*. In the low-momentum regime ($p \ll \mathcal{M}$), Weldon has obtained approximate expressions for the dispersion relation of each of the modes [8]:

$$p_0 \;=\; \overset{+}{\scriptstyle(-)}\, E^{p\,(\bar{p})} \;\approx\; \overset{+}{\scriptstyle(-)} \left[\mathcal{M} + \frac{p}{3} + \frac{p^2}{3\mathcal{M}} + \cdots\right] \tag{4.16a}$$

$$p_0 \;=\; \overset{+}{\scriptstyle(-)}\, E^{h\,(\bar{h})} \;\approx\; \overset{+}{\scriptstyle(-)} \left[\mathcal{M} - \frac{p}{3} + \frac{p^2}{3\mathcal{M}} + \cdots\right], \tag{4.16b}$$

with

[1]All numerical calculations in the present work were performed using *Mathematica*, as well as the plotting of the results.

$$\mathcal{M} \;=\; p_0(\mathbf{p}=0) \;=\; \frac{eT}{2\sqrt{2}}. \tag{4.17}$$

In particular, results (4.16) show that we have $E^{(p)} = E^{(\bar{p})}$ and $E^{(h)} = E^{(\bar{h})}$. Furthermore, we see that the interaction of the massless electrons with the thermal bath generates a finite thermal mass $\mathcal{M}$. Its value (4.17) may be obtained straightforwardly by solving the dispersion relation (4.12) with $|\mathbf{p}| = 0$, using the values of a, b given in (4.15). In fig. 4.5(b), the dispersion relations of the excitations are compared with that of a free fermion of mass $\mathcal{M}$. It was shown by Weldon [7] that although the dotted curve is always an underestimate of $E^{(p)}$, the error is never larger than 10%. This confirms $\mathcal{M}$ as an approximate thermal mass for the thermalised electrons and positrons.

We shall now discuss the meaning of the hole excitations, given by the inner curves in fig. 4.5.

4.5 (Anti)particle and (anti)hole excitations

Zero-temperature spinors

In order to interpret the spectrum given by the dispersion relation in the previous section, we must analyse the solutions of the Dirac equation. We will start with the case of a vacuum. As we have discussed earlier, in quantum field theory a propagating particle is described by a field operator of the form

$$\psi(t, \mathbf{x}) = e^{-i(p_0 t - \mathbf{k}\cdot\mathbf{x})}\psi_0, \tag{4.18}$$

where ψ_0 is a time-independent wavefunction that is made to propagate as a plane wave due to the exponential function in front. For an electron field in a vacuum (we will include a mass term m for generality), finding the wavefunction amounts to solving the Dirac equation

$$(\not{k} - m)\psi_0 \;\equiv\; (\gamma^0 p_0 - \boldsymbol{\gamma}\cdot\mathbf{k} - m)\psi_0 \;=\; 0 \tag{4.19}$$

which as we know has two solutions, $p_0 = E^{(p)} = \sqrt{\mathbf{p}^2 + m^2}$ and $p_0 = -E^{(p)} = -\sqrt{\mathbf{p}^2 + m^2}$, with $E^{(p)} = E^{(\bar{p})}$ (the exponent $p\,(\bar{p})$ stands for *(anti)particle*). Upon substitution of these energy solutions into the Dirac equation (4.19), we obtain the following wavefunctions, represented here using the chiral base[2] of the Dirac matrices [25]:

$$\begin{aligned}(\gamma^0 E^{(p)} - \boldsymbol{\gamma}\cdot k - m)\psi_0 =&0\\ \Longrightarrow \psi_0 =& \begin{pmatrix} \mathbb{1} + \frac{\boldsymbol{\sigma}\cdot\mathbf{p}}{E^{(p)}+m} \\ -\mathbb{1} + \frac{\boldsymbol{\sigma}\cdot\mathbf{p}}{E^{(p)}+m}\end{pmatrix} \chi^\lambda(\mathbf{p}) \qquad (p_0 = E^{(p)},\ \mathbf{p}=\mathbf{k}) \qquad (4.20a)\\ (-\gamma^0 E^{(\bar{p})} - \boldsymbol{\gamma}\cdot k - m)\psi_0 =&0\\ \Longrightarrow \psi_0 =& \begin{pmatrix} \mathbb{1} - \frac{\boldsymbol{\sigma}\cdot\mathbf{p}}{E^{(\bar{p})}+m} \\ \mathbb{1} + \frac{\boldsymbol{\sigma}\cdot\mathbf{p}}{E^{(\bar{p})}+m}\end{pmatrix} \chi^\lambda(\mathbf{p}) \qquad (p_0 = -E^{(\bar{p})},\ \mathbf{p}=-\mathbf{k}) \qquad (4.20b)\end{aligned}$$

where $\mathbb{1}$ is the 2×2 unit matrix, $\boldsymbol{\sigma} = \sigma_i$ are the three Pauli matrices and $\chi^\lambda(\mathbf{p})$ is a normalised two-component spinor, which is an eigenstate of the momentum $\mathbf{p}$. At the same time, for the purpose of this discussion, we will choose the spinor χ to be an eigenstate of the spin projection along the direction of motion, i.e. a *helicity* eigenstate:

$$(\boldsymbol{\Sigma}\cdot\hat{\mathbf{k}})\ \chi^\lambda(\hat{\mathbf{k}}) = \begin{pmatrix} \boldsymbol{\sigma}\cdot\hat{\boldsymbol{k}} & 0 \\ 0 & \boldsymbol{\sigma}\cdot\hat{\boldsymbol{k}}\end{pmatrix} \chi^\lambda(\hat{\mathbf{k}}) = \lambda\ \chi^\lambda(\hat{\mathbf{k}}), \qquad (4.21)$$

where $\lambda = \pm 1$ is the corresponding helicity eigenvalue (so that the spin projection $S_{\hat{k}} = \frac{1}{2}\boldsymbol{\Sigma}\cdot\hat{\mathbf{k}}$ has eigenvalues $\pm 1/2$). We may then rewrite the wavefunctions (4.20) as

$$\begin{aligned}u_p(\mathbf{p},\lambda) &= \begin{pmatrix} \mathbb{1} + \frac{\lambda|\mathbf{p}|}{E^{(p)}+m} \\ -\mathbb{1} + \frac{\lambda|\mathbf{p}|}{E^{(p)}+m}\end{pmatrix} \chi^\lambda(\mathbf{p}) \qquad (p_0 = E^{(p)},\ \mathbf{p}=\mathbf{k})\\ v_{\bar{p}}(-\mathbf{p},\lambda) &= \begin{pmatrix} \mathbb{1} - \frac{\lambda|\mathbf{p}|}{E^{(\bar{p})}+m} \\ \mathbb{1} + \frac{\lambda|\mathbf{p}|}{E^{(\bar{p})}+m}\end{pmatrix} \chi^\lambda(\mathbf{p}) \qquad (p_0 = -E^{(\bar{p})},\ \mathbf{p}=-\mathbf{k})\end{aligned} \qquad (4.22)$$

and upon substitution in (4.18), we obtain the field solutions

$$\begin{aligned}\psi_p(t,\mathbf{x}) &= e^{-i(E^{(p)}t - \mathbf{p}\cdot\mathbf{x})} u_p(\mathbf{p},\lambda) \qquad (p_0 = E^{(p)},\ \mathbf{p}=\mathbf{k})\\ \psi_{\bar{p}}(t,\mathbf{x}) &= e^{i(E^{(\bar{p})}t - (-\mathbf{p})\cdot\mathbf{x})} v_{\bar{p}}(-\mathbf{p},\lambda) \quad (p_0 = -E^{(p)},\ \mathbf{p}=-\mathbf{k})\end{aligned} \qquad (4.23)$$

[2]In the chiral base the Dirac matrices are written $\gamma^0 = \begin{pmatrix} 0 & -\mathbb{1} \\ -\mathbb{1} & 0\end{pmatrix}$, $\boldsymbol{\gamma} = \begin{pmatrix} 0 & \boldsymbol{\sigma} \\ -\boldsymbol{\sigma} & 0\end{pmatrix}$ [25].

where the positive-energy solution represents an electron in the initial state (i.e. its annihilation at point $t, \mathbf{x}$) with momentum $\mathbf{p}$, helicity λ and energy $E^{(p)}$, and the other represents an positron in the final state (i.e. its creation) with momentum $-\mathbf{p}$, helicity λ and the *same* energy $E^{(\bar{p})} = E^{(p)}$.

In the limit $m \to 0$ we have $\frac{\lambda|\mathbf{p}|}{E+m} \to \frac{\lambda|\mathbf{p}|}{E} = 1$, and thus the spinors (4.22) become

$$\begin{aligned}
\lambda = +1 : \quad u_p(\mathbf{p}, +1) &\propto \begin{pmatrix} \mathbb{1} \\ 0 \end{pmatrix} \chi^+(\mathbf{p}) \qquad (\mathbf{p} = \mathbf{k}) \\
v_{\bar{p}}(-\mathbf{p}, +1) &\propto \begin{pmatrix} 0 \\ \mathbb{1} \end{pmatrix} \chi^+(\mathbf{p}) \qquad (\mathbf{p} = -\mathbf{k}) \\
\lambda = -1 : \quad u_p(\mathbf{p}, -1) &\propto \begin{pmatrix} 0 \\ \mathbb{1} \end{pmatrix} \chi^-(\mathbf{p}) \qquad (\mathbf{p} = \mathbf{k}) \\
v_{\bar{p}}(-\mathbf{p}, -1) &\propto \begin{pmatrix} \mathbb{1} \\ 0 \end{pmatrix} \chi^-(\mathbf{p}) \qquad (\mathbf{p} = -\mathbf{k})
\end{aligned} \tag{4.24}$$

We see that the solutions with positive helicity ($\lambda = +1$) also have positive chirality[3], and those with negative helicity ($\lambda = -1$) have negative chirality.

These four fields (taking into account the two possible helicity eigenstates of each spinor) form a complete set of solutions of the free Dirac equation in a vacuum. We shall now see how the inclusion of a thermal medium allows for multiple solutions, in order to interpret the plot of fig. 4.5.

Finite-temperature spinors: particles and holes

As discussed throughout this chapter, the inclusion of a medium at finite temperature and density will yield corrections to the Dirac equation, which (for massless fermions) were represented by the parameters a and b (cf. (4.12)). However, these corrections may be represented equally well by a different set of temperature-dependent parameters, and for the present discussion we will define the parameters $n(p_0, \mathbf{p})$ and $m(p_0, \mathbf{p})$ as follows:

---

[3]Chirality eigenstates obey $\gamma_5\psi = \pm\psi$. In the chiral base we have $\gamma_5 = \begin{pmatrix} \mathbb{1} & 0 \\ 0 & -\mathbb{1} \end{pmatrix}$. Thus, in this base the chirality eigenstates are given by $\begin{pmatrix} \mathbb{1} & 0 \\ 0 & -\mathbb{1} \end{pmatrix}\begin{pmatrix} \mathbb{1} \\ 0 \end{pmatrix} = +\begin{pmatrix} \mathbb{1} \\ 0 \end{pmatrix}$ (positive chirality), and $\begin{pmatrix} \mathbb{1} & 0 \\ 0 & -\mathbb{1} \end{pmatrix}\begin{pmatrix} 0 \\ \mathbb{1} \end{pmatrix} = -\begin{pmatrix} 0 \\ \mathbb{1} \end{pmatrix}$ (negative chirality).

$$\begin{aligned} \left[\gamma^0 p_0 - \boldsymbol{\gamma}\cdot\mathbf{p} - m\right]\psi_0 &= 0 \qquad (T=0) \\ \left[\gamma^0 n(p_0,\mathbf{p})p_0 - \boldsymbol{\gamma}\cdot\mathbf{p} - m(p_0,\mathbf{p})\right]\psi_0 &= 0 \qquad (T\neq 0) \end{aligned} \tag{4.25}$$

so that $m(p_0,\mathbf{p})$ may be interpreted as an effective thermal mass, and $n(p_0,\mathbf{p})$ as a refractive index. These corrections will shift the solutions of the Dirac equation (4.25) from $p_0 = \pm\sqrt{\mathbf{p}^2+m^2}$ to

$$p_0\, n(p_0,\mathbf{p}) \;=\; \pm\sqrt{\mathbf{p}^2+m^2(p_0,\mathbf{p})} \;=\; \pm\,\varepsilon(p_0,\mathbf{p}) \implies p_0 \;=\; \frac{\pm\,\varepsilon(p_0,\mathbf{p})}{n(p_0,\mathbf{p})} \tag{4.26}$$

where $\varepsilon(p_0,\mathbf{p})$ has an identical form to the energy of a free particle, but depends on the thermal parameter $m(p_0,\mathbf{p})$ and not simply on the free mass m. One consequence that is immediately evident is that the particle and antiparticle energies need not be equal, while in a vacuum they must be so by TCP invariance.

As we will show next, one may obtain different solutions for each sign of p_0 by considering either positive or negative values of n; to the solutions with $n > 0$ one calls *particles* or *antiparticles* (for $p_0 > 0$ and $p_0 < 0$, respectively), while to the ones obtained with values of $n < 0$ one calls *holes* or *anti-holes* (for $p_0 > 0$ and $p_0 < 0$, respectively). These last solutions will be shown to possess a different relation between helicity and chirality than particles and antiparticles.

First, suppose a solution for $p_0 = E^{(p)} > 0$, obtained by a positive value of n, i.e. $n(E^{(p)},\mathbf{p}) = n^{(p)} > 0$. At the same time, consider also a solution of the antiparticle type i.e. for $p_0 = -E^{(\bar{p})} < 0$ and, again, positive $n = n^{(\bar{p})}$. Note that the energies may be written

$$E^{(p)} = \frac{+\varepsilon^{(p)}}{n^{(p)}} > 0, \quad E^{(\bar{p})} = \frac{+\varepsilon^{(\bar{p})}}{n^{(\bar{p})}} > 0. \tag{4.27}$$

Substitution of each set of variables in the modified Dirac's equation (4.25) will lead to the following particle and antiparticle wavefunctions:

$$
\begin{aligned}
u_p(\mathbf{p},\lambda) &= \begin{pmatrix} \mathbb{1} + \frac{\lambda|\mathbf{p}|}{\varepsilon^{(p)}+m^{(p)}} \\ -\mathbb{1} + \frac{\lambda|\mathbf{p}|}{\varepsilon^{(p)}+m^{(p)}} \end{pmatrix} \chi^\lambda(\mathbf{p}) \qquad (p_0 > 0, n_p > 0) \\
v_{\bar{p}}(-\mathbf{p},\lambda) &= \begin{pmatrix} \mathbb{1} - \frac{\lambda|\mathbf{p}|}{\varepsilon^{(\bar{p})}+m^{(\bar{p})}} \\ \mathbb{1} + \frac{\lambda|\mathbf{p}|}{\varepsilon^{(\bar{p})}+m^{(\bar{p})}} \end{pmatrix} \chi^\lambda(\mathbf{p}) \qquad (p_0 < 0, n_{\bar{p}} > 0)
\end{aligned} \tag{4.28}
$$

which, by (4.18), will propagate through the thermal medium according to[4]

$$
\begin{aligned}
\psi(t,\mathbf{x}) =& e^{-i(E^{(p)}t-\mathbf{p}\cdot\mathbf{x})} u_p(\mathbf{p},\lambda) \qquad (p_0 > 0,\ n_p > 0) \\
\psi(t,\mathbf{x}) =& e^{i[E^{(\bar{p})}t-(-\mathbf{p})\cdot\mathbf{x}]} v_{\bar{p}}(-\mathbf{p},\lambda) \qquad (p_0 < 0,\ n_p > 0)
\end{aligned} \tag{4.29}
$$

These fields, like their zero-temperature equivalents (4.23), represent respectively the destruction of a particle and the creation of an antiparticle, with momentum $\mathbf{p}$ and $-\mathbf{p}$; however, in contrast with the zero-temperature case, they have energies $E^{(p)} = \varepsilon^{(p)}/n^{(p)}$ and $E^{(\bar{p})} = -\varepsilon^{(\bar{p})}/n^{(\bar{p})}$. This allows for the possibility that they have different energies from each other, if it be the case that $m^{(p)} \neq m^{(\bar{p})}$ or $n^{(p)} \neq n^{(\bar{p})}$.

According to our results expressed in fig. 4.5, at finite temperature there must be another pair of solutions arising from Dirac's equation. We will then look for qualitatively different solutions by using *negative* values of the 'refractive index' n. Suppose one solution for a certain positive $p_0 = E^{(h)} > 0$, possessing $n^{(h)} = n(E^{(h)},\mathbf{p}) < 0$; and another solution having $p_0 = -E^{(\bar{h})} < 0$ and also a negative value of $n = n^{(\bar{h})} < 0$. This time, the energies of these solutions will be written

$$
E^{(h)} = \frac{-\varepsilon^{(h)}}{n^{(h)}} > 0, \quad E^{(\bar{h})} = \frac{-\varepsilon^{(\bar{h})}}{n^{(\bar{h})}} > 0, \tag{4.30}
$$

because we have established that $n < 0$.

Solving the respective thermal Dirac equations (4.25), we obtain the wavefunctions

$$
\begin{aligned}
u_h(\mathbf{p},\lambda) &= \begin{pmatrix} \mathbb{1} - \frac{\lambda|\mathbf{p}|}{\varepsilon^{(\bar{p})}+m^{(\bar{p})}} \\ \mathbb{1} + \frac{\lambda|\mathbf{p}|}{\varepsilon^{(\bar{p})}+m^{(\bar{p})}} \end{pmatrix} \chi^\lambda(\mathbf{p}) \qquad (p_0 > 0,\ n^{(h)} < 0) \\
v_{\bar{h}}(-\mathbf{p},\lambda) &= \begin{pmatrix} \mathbb{1} + \frac{\lambda|\mathbf{p}|}{\varepsilon^{(\bar{p})}+m^{(\bar{p})}} \\ -\mathbb{1} + \frac{\lambda|\mathbf{p}|}{\varepsilon^{(\bar{p})}+m^{(\bar{p})}} \end{pmatrix} \chi^\lambda(\mathbf{p}) \qquad (p_0 < 0,\ n^{(\bar{h})} < 0),
\end{aligned} \tag{4.31}
$$

[4]Note these solutions depend on the thermodynamics of the medium through the finite-temperature corrections $n(p_0,\mathbf{p})$ and $m(p_0,\mathbf{p})$.

which have a different form from either u_p or $v_{\bar{p}}$ (cf. (4.28)). To the first solution we shall call a *hole* wavefunction and to the second an *anti-hole* [8]. In the massless limit, these spinors yield

$$\begin{aligned}
\lambda = +1: \quad & u_p(\mathbf{p}, +1) \propto \begin{pmatrix} 0 \\ \mathbb{1} \end{pmatrix} \chi^+(\mathbf{p}) \qquad (\mathbf{p} = \mathbf{k}) \\
& v_{\bar{p}}(-\mathbf{p}, +1) \propto \begin{pmatrix} \mathbb{1} \\ 0 \end{pmatrix} \chi^+(\mathbf{p}) \qquad (\mathbf{p} = -\mathbf{k}) \\
\lambda = -1: \quad & u_p(\mathbf{p}, -1) \propto \begin{pmatrix} \mathbb{1} \\ 0 \end{pmatrix} \chi^-(\mathbf{p}) \qquad (\mathbf{p} = \mathbf{k}) \\
& v_{\bar{p}}(-\mathbf{p}, -1) \propto \begin{pmatrix} 0 \\ \mathbb{1} \end{pmatrix} \chi^-(\mathbf{p}) \qquad (\mathbf{p} = -\mathbf{k})
\end{aligned} \tag{4.32}$$

whence the solutions with positive helicity ($\lambda = +1$) have negative chirality and those with negative helicity ($\lambda = -1$) have positive chirality.

We thus conclude that the solutions of the thermal Dirac equation with a value of $n(p_0, |\mathbf{p}|) < 0$, which we call 'holes' and 'antiholes', have the an opposite relation between helicity and chirality, in the massless limit. As we saw, this is never the case for electrons nor positrons, either in a vacuum or in a thermal medium.

For completeness, we present the field operators of holes and anti-holes, which include the spinors discussed above:

$$\begin{aligned}
\psi_h(t, \mathbf{x}) =& e^{-i(E^{(h)}t - \mathbf{p}\cdot\mathbf{x})} u_h(\mathbf{p}, \lambda), \\
\psi_{\bar{h}}(t, \mathbf{x}) =& e^{i(E^{(\bar{h})}t - (-\mathbf{p})\cdot\mathbf{x})} v_{\bar{h}}(-\mathbf{p}, \lambda),
\end{aligned} \tag{4.33}$$

which represent respectively the destruction of a hole of momentum $\mathbf{p}$, helicity λ and energy $E^{(h)}$, and the creation of an anti-hole of momentum $-\mathbf{p}$, helicity λ and energy $E^{(\bar{h})}$.

Chapter 5

The degenerate electron plasma

5.1 Description of the system

In the previous chapter we discussed the collective behaviour arising from the self-energy correction in a high-temperature plasma. The literature we reviewed considered a plasma of massless particles with the same number of fermions as anti-fermions. Should such system be brought to low temperatures, pair annihilation would inevitably dominate over pair production as the average distance between particles decreased and in the zero-temperature limit all particle pairs would annihilate, turning the system into a vacuum. This feature is mathematically inbuilt in the Fermi-Dirac distribution with zero chemical potential (4.1):

$$n_F(p) = \frac{1}{e^{\beta E_p} + 1} \xrightarrow{(\beta \to \infty)} 0 \tag{5.1}$$

However, this will not be the case if there is an asymmetry between the fermion and antifermion distributions, which may be formalised by a finite chemical potential μ. In that case, in the zero temperature limit, upon thorough annihilation of the available pairs, there will subsist a degenerate distribution of either fermions or antifermions:

$$n_F(p) = \frac{1}{e^{\beta(E_p \mp \mu)} + 1} \xrightarrow{(\beta \to \infty)} \theta(\mu - E_p) = \begin{cases} 0 \quad , & E_p > \mu \\ 1 \quad , & E_p < \mu \end{cases} \tag{5.2}$$

From this result we deduce that the chemical potential of a degenerate distribution is its Fermi energy, $\mu = E_F$, defined as the maximum energy of a particle of the distribution in the ground state[1]. One then defines the Fermi momentum p_F by the relativistic relation $E_F = \sqrt{p_F^2 + m^2}$.

In the present chapter we will explore the case of a degenerate distribution of electrons. Unlike previously, we will consider a finite electron mass m that will break the chiral symmetry of the system. The finite electron mass will represent an additional energy scale in the problem; at the same time, by taking the limit $T \to 0$ we may no longer use temperature as an energy scale characterising the medium; instead, this role is now played by the Fermi energy or, equivalently, the Fermi momentum.

In order to make reasonable estimates, we will base our discussion on the example of the core of a neutron star. To that end, we must first relate the abstract concept of Fermi momentum with that of particle density. The density of quantum states of a fermion in a volume V is [26]

$$G(|\mathbf{p}|)d|\mathbf{p}| = 2 \cdot \frac{V}{(2\pi)^3} \cdot 4\pi \mathbf{p}^2 d|\mathbf{p}|, \tag{5.3}$$

where the factor of 2 accounts for the degenerate spin states. The number of fermions N is obtained by integration of the density of states up to the Fermi energy:

$$N = \frac{V}{\pi^2} \int_0^{p_F} \mathbf{p}^2 d|\mathbf{p}| = \frac{V p_F^3}{3\pi^2} \tag{5.4}$$

$$\implies p_F = \left(3\pi^2 \frac{N}{V}\right)^{1/3}$$

$$= \left(3\pi^2 n\right)^{1/3} \tag{5.5}$$

yielding the desired relation between the Fermi momentum and the electron density n. Knowing that the chemical equilibrium in the star among neutrons (n), electrons (e) and protons (p) is given by [16]

$$E_{F,n} = E_{F,e} + E_{F,p} = \sqrt{p_{F,e}^2 + m_e^2} + \sqrt{p_{F,p}^2 + m_p^2}, \tag{5.6}$$

we may try to estimate the Fermi momentum of the electron distribution. The core of a neutron star has a density of five to ten times that of normal nuclear matter [16]; if

[1] Moreover, note that if one adds a particle to a degenerate plasma with large total energy E and total number of particles N, its total energy will increase by $E_F + \delta E \approx E_F$, which shows that in the thermodynamic limit the Fermi energy satisfies the thermodynamic definition of chemical potential, $E_F = \mu = (\partial E/\partial N)_V$.

we use for the latter the value $n_0 = 0.15$ nucleons per fm^3 [4], and suppose a neutron star core five times denser ($n = 0.75$ fm^{-3}), we obtain by eq. (5.5)

$$p_{F,n} = \left(3\pi^2 \times 0.75 \text{ fm}^{-3}\right)^{1/3} \times 197 \text{ MeV} \cdot \text{fm} \ \approx 550 \text{ MeV} \tag{5.7}$$

Moreover, the condition of charge neutrality of the star implies $p_{F,e} = p_{F,p}$. Relation (5.6) then yields (considering $m_n \approx m_p \approx 940$ MeV)

$$\begin{aligned} E_{F,n} \text{ (MeV)} \ = \ \sqrt{p_{F,n}^2 + m_n^2} \ &= \sqrt{p_F^2 + m_e^2} + \sqrt{p_F^2 + m_p^2} \\ \sqrt{550^2 + 940^2} \ &= \sqrt{p_F^2 + 0.5^2} + \sqrt{p_F^2 + 940^2} \\ &\approx p_F + \sqrt{p_F^2 + 940^2} \\ \Longrightarrow \ p_F \ &\approx 140 \text{ MeV} \end{aligned} \tag{5.8}$$

where p_F is the Fermi momentum of the electron and proton distributions.

We may thus consider an order of magnitude of $p_F \sim 100$ MeV $= 200\ m_e$ for the electron distribution in the core of a neutron star. This ratio will be used in our analysis, particularly in plotting the results. Note that by eq. (5.5), this corresponds to an electron density of the order of 10^{37} cm^{-3}, around 10^{14} times larger than that of a metal at room temperature [27].

Although a neutron star starts as a relatively warm body upon collapse of a supernova core, possibly with a temperature of around 10 to 40 MeV [4, 17], upon neutrino emission it eventually cools down to less than 1 MeV [16]. In this state, the electron distribution satisfies $T \ll p_F$ and the zero-temperature approximation may thus be applied. This justifies our treatment of the electron distribution as degenerate.

5.2 Thermal self-energy of massive electrons

In parallel with the self-energy structure for a chirally invariant system (4.6), for a plasma of massive electrons we may now write

$$\Sigma_\beta(p, u) = -a\not{p} - b\not{u} - c \tag{5.9}$$

The parameters $a(p_0, |\mathbf{p}|)$ and $b(p_0, |\mathbf{p}|)$ correspond to the projection of Σ_β onto $\not{p}$ and $\not{u}$ respectively, as in the chirally invariant system of the previous chapter (cf. (4.13)), while the parameter we have named $c(p_0, |\mathbf{p}|)$ is the projection of the self-energy on the unit matrix:

$$c = -\frac{1}{4}\,\mathrm{tr}\,\Sigma_\beta. \tag{5.10}$$

For the system of the previous chapter, the electron propagator (3.28) depended only on $\not{p}$ and on $p_0 = p \cdot u = \frac{1}{4}\,\mathrm{tr}\,\not{p}\not{u}$, because the electron mass was set to zero. Therefore, the projections of the self-energy on $\not{p}$ and $\not{u}$ were sufficient for its description. On the other hand, in the present case the self-energy must depend also on the parameter c because the electron propagator depends additionally on the free mass m. Hence, c is a scalar that parametrises the chirality violation.

Inserting the self-energy form (5.9) in the dressed thermal propagator, we obtain

$$\begin{aligned} S(p,u) =& \frac{1}{\not{p} - m - \Sigma(p,u) + i\epsilon} \\ =& \frac{1}{(1+a)\not{p} + b\not{u} - (m-c) + i\epsilon} \\ =& \frac{(1+a)\not{p} + b\not{u} + m - c}{(1+a)^2p^2 + b^2u^2 + 2(1+a)bp\cdot u - (m-c)^2}. \end{aligned} \tag{5.11}$$

As discussed previously, the zeros of the denominator yield the dispersion relation of the propagation modes:

$$\begin{aligned} (1+a)^2p^2 + b^2 + 2(1+a)bp\cdot u - (m-c)^2 =& 0 \\ [(1+a)p_0 + b]^2 - (1+a)^2\mathbf{p}^2 - (m-c)^2 =& 0 \\ \equiv \mathcal{F}(p_0, |\mathbf{p}|) =& 0. \end{aligned} \tag{5.12}$$

Note that the inclusion of a mass term has made it impossible to factor the expression explicitly as was done in the previous chapter (cf. (4.12)).

Substituting the degenerate distribution (5.2) in the thermal propagator (4.8), we obtain for the T-dependent part of the self-energy loop (note that $\gamma^\mu\gamma_\mu = 4$ and, as before, $\gamma^\mu \not{p} \gamma_\mu = -2\not{p}$):

$$\begin{aligned}\Sigma_\beta =& ie'^2 \int \frac{d^4p'}{(2\pi)^4} \frac{\gamma^\mu(\not{p}' + m)\gamma_\mu}{(p-p')^2} n_F(|\mathbf{p}'|)\theta(p'_0)2\pi\delta(p'^2 - m^2) \\ =& -2e^2 \int \frac{d^4p'}{(2\pi)^4} \frac{\not{p}' - 2m}{(p-p')^2} \theta(p_F - |\mathbf{p}'|) \frac{2\pi\delta(p'_0 - E_{p'})}{2E_{p'}} \\ =& e^2 \int \frac{d^3p'}{(2\pi)^3} \frac{1}{E_{p'}} \frac{-\not{p}' + 2m}{p^2 + m^2 - 2p_0E_{p'} + 2|\mathbf{p}||\mathbf{p}'|\cos\theta} \theta(p_F - |\mathbf{p}'|),\end{aligned} \tag{5.13}$$

The inclusion of the Heaviside function $\theta(p'_0)$ in the first line is meant to assure that only electrons rather than positrons are considered.

5.3 Results and discussion

Because of the complexity of the analytic results obtained we will refer the reader to appendix D for consultation.

Firstly, the projections of the integral (5.13) defined in (5.9) are developed in appendix D.1. Because of the degenerate distribution function, that limits the integration in $d|\mathbf{p}'|$ to the range $0 < |\mathbf{p}'| < p_F$, these integrations may be performed analytically, and we have therefore been able to obtain exact expressions for a, b and c, which may be consulted in appendix D.2.

By substitution of the exact results into (5.12) an implicit form of the dispersion relation may be derived[2]. The dispersion relation has been plotted in fig. 5.1 for a Fermi momentum of $p_F = 200\,m$, where dashed lines have been added representing $p_0 = \pm|\mathbf{p}|$.

One characteristic in which the dispersion relation differs from that of the previous chapter is the appearance of six solutions, rather than four; however, the two innermost curves, labelled E_τ and $E_{\bar{\tau}}$, are entirely in the space-like region $|\mathbf{p}| > |p_0|$ delimited by the dashed lines, and it has been checked that they approach the limit of the region asymptotically. Therefore, these solutions correspond to unstable modes and shall be ignored because they are outside the scope of this study. This leaves us once again with

[2]The dispersion relation cannot be calculated in an explicit form of the kind $p_0 = p_0(p)$ because the logarithmic functions resulting from the integration render the expression transcendental.

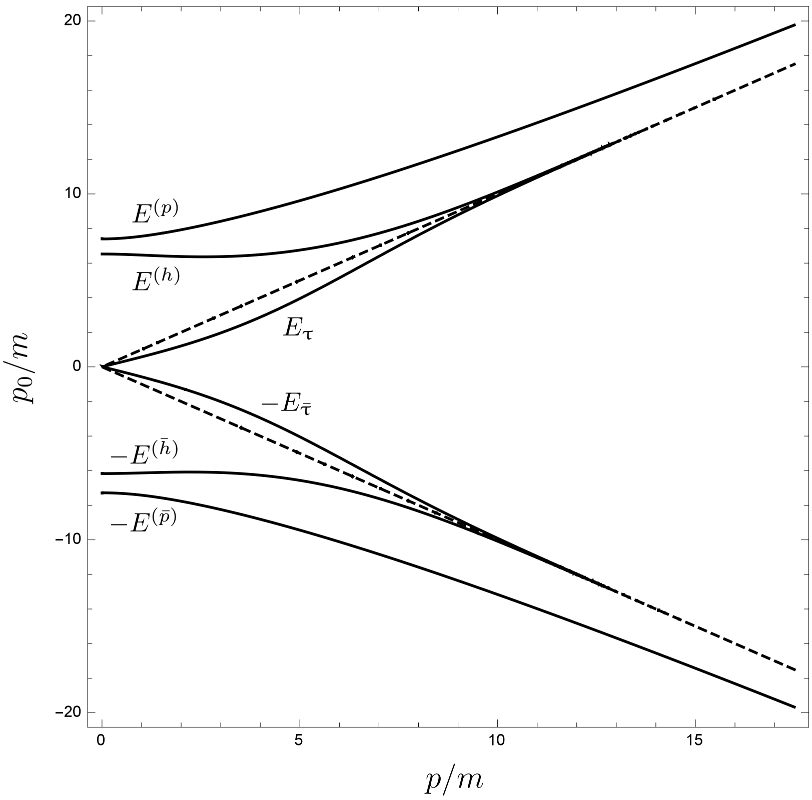

FIGURE 5.1: Plot of the dispersion relation (5.12), using the exact values of a, b, c obtained analytically, as displayed in appendix D.2, using $p_F = 200\,m$. The dashed lines represent $p_0 = \pm|\mathbf{p}|$, and thus separate the time- and space-like regions.

four physical solutions lying in the time-like region, as had been found for the chirally invariant, high-T plasma of Chap. 4.

We shall now analyse these solutions, and discuss some of their properties.

5.3.1 Rest energy of the fermionic modes

Taking the limit $p \to 0$, the dispersion relation (5.12) becomes

$$\begin{aligned} \mathcal{F}(p_0, |\mathbf{p}| = 0) = [(1+a)p_0 + b]^2 - (m-c)^2 &= 0 \\ [(1+a)p_0 + b - m + c][(1+a)p_0 + b + m - c] &= 0 \\ \mathcal{F}_1(p_0)\mathcal{F}_2(p_0) &= 0. \end{aligned} \tag{5.14}$$

As we may see, the dispersion relation may now be factored because the term $(1+a)|\mathbf{p}|$ vanishes. Therefore, it may be rewritten as two distinct conditions:

$$\mathcal{F}_{1\,(2)}(p_0) \;=\; (1+a)p_0 \mp m + b \pm c \;=\; 0 \tag{5.15}$$

Because we are considering a regime with $p_F \gg m$, and since the rest energy of each of the solutions is given by a small correction to the electron mass, we may therefore consider $p_F \gg p_0$ $(p=0)$. In that approximation, the dispersion relation (5.15) yields (see appendix D.3):

$$\begin{aligned} \mathcal{F}_{1\,(2)}(p_0) \;&=\; p_0 \mp m - \frac{\alpha}{2\pi}\frac{p_F E_F}{p_0} \;=0 \\ &\approx\; p_0 \mp m - \frac{\alpha}{2\pi}\frac{p_F^2}{p_0} \;=0, \end{aligned} \tag{5.16}$$

where the last approximation is allowed because of $p_F \gg m$.

The dispersion relations (5.16) may then be rewritten in terms of the rest energy:

$$\begin{aligned} p_0(|\mathbf{p}|=0) \;&=\; \frac{m}{2} \pm \sqrt{\left(\frac{m}{2}\right)^2 + \frac{\alpha}{2\pi}p_F^2} \qquad (\mathcal{F}_1 = 0) \\ p_0(|\mathbf{p}|=0) \;&=-\; \frac{m}{2} \pm \sqrt{\left(\frac{m}{2}\right)^2 + \frac{\alpha}{2\pi}p_F^2} \qquad (\mathcal{F}_2 = 0) \end{aligned} \tag{5.17}$$

The rest energies of the (anti)particle states are those that obey $\lim_{p_F\to 0}(p_0) = \pm m$, namely the positive solution of $\mathcal{F}_1$ and the negative solution of $\mathcal{F}_2$. For the other two solutions, we may easily see that $\lim_{p_F\to 0}(p_0) = 0$. Therefore, they must correspond to the (anti-)hole states, which do not exist in a vacuum.

For values of $p_F \gg m$, it may easily be checked that the mass term in the square root may me neglected in comparison with the Fermi momentum term. Performing the latter approximation, we obtain

$$\begin{aligned} p_0(|\mathbf{p}|=0) \;&\approx \pm\sqrt{\frac{\alpha}{2\pi}}p_F \pm \frac{m}{2} \qquad \text{electron (positron)} \\ p_0(|\mathbf{p}|=0) \;&\approx \pm\sqrt{\frac{\alpha}{2\pi}}p_F \mp \frac{m}{2} \qquad \text{hole (anti-hole)} \end{aligned} \tag{5.18}$$

Thus, to leading order in p_F, the consequence of the finite electron mass is a different value of rest energy for the electron and the hole solutions. acquire from each other, which would not be the case if the system had chiral invariance:

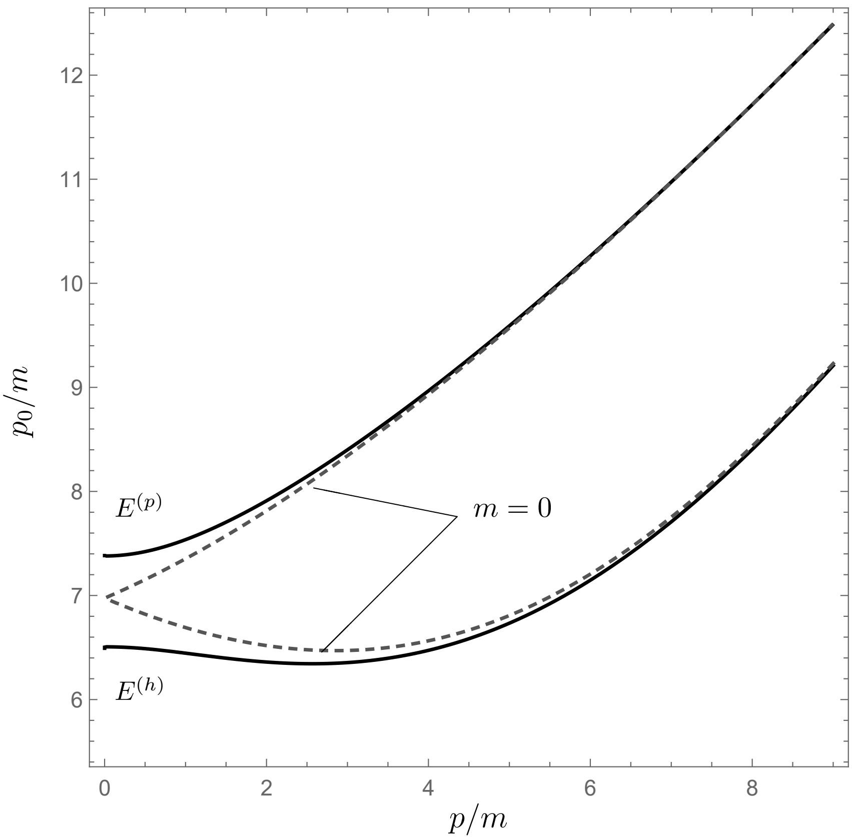

FIGURE 5.2: Solid lines: exact dispersion relation of the electron $E^{(p)}$ and hole $E^{(h)}$ modes in a degenerate electron plasma with Fermi momentum $p_F = 200\,m$. Dashed lines: dispersion relation of the same modes for $m = 0$.

$$p_0\left(|\mathbf{p}| = m = 0\right) = \frac{\alpha}{2\pi}p_F^2 \tag{5.19}$$

We see from (5.18) and (5.19) that the rest energy of the electron mode has an approximate increase of half an electron mass compared with the chirally invariant case, while the rest energy of the hole decreases by half an electron mass. This creates a gap in the mass spectrum of the system between electrons and holes, whose approximate value is the electron mass. This result is illustrated in fig. 5.2.

5.3.2 Comparison between electron/positron and hole/anti-hole dispersion relations

Although to leading order in p_F (5.18) the electron and positron have the same energy, as well as the hole and anti-hole, by plotting the exact dispersion relation as in fig. 5.1 we may see there is in fact a difference between the dispersion relations of electron and

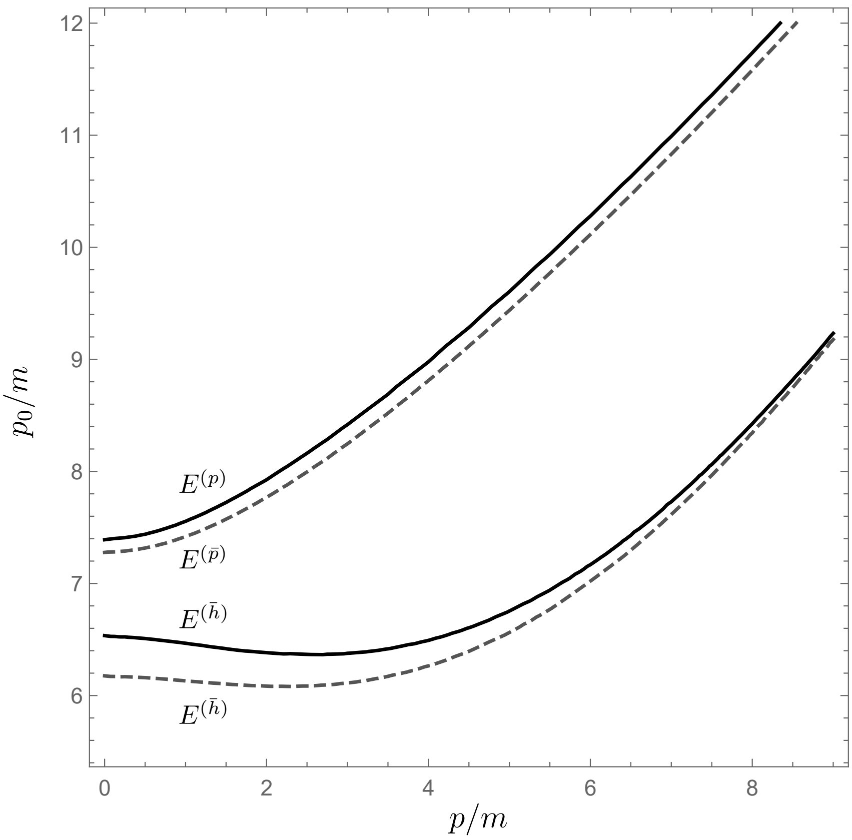

Figure 5.3: Exact dispersion relation of the four fermionic modes of a degenerate electron plasma with Fermi momentum $p_F = 200\,m$. We have plotted the absolute value of the solutions for a better comparison.

positron, as well as between hole and anti-hole. This feature may be seen in the plot of fig. 5.3.

This feature was not present in the system studied in Chap. 4. The reason for its occurrence in the present case is the asymmetry of the plasma, which contains only electrons, rather than positrons. On the other hand, the previous system had exact matter/antimatter symmetry, and the solutions were symmetrically disposed.

5.3.3 Comparison with a chirally invariant symmetric plasma

Lastly, we will check the validity of our results by comparing them with those obtained by Weldon (Chap. 4). To that end, we must adapt the expressions for the self-energy, eq. (D.4), to a symmetric plasma of massless electrons and positrons, allowing for a direct comparison with the system of the previous chapter. This may be done by adding to the degenerate distribution of electrons a distribution of positrons with the same Fermi momentum p_F. It has been checked explicitly that the self-energy correction of an electron in a *positron* plasma may be obtained from that of an electron in an *electron* plasma by means of the substitution $E_F, p_F \to -E_F, -p_F$. The resulting expressions are presented in eq. (D.8). These expressions must now be added to (D.2) in order to obtain a symmetric degenerate plasma. This was also performed in the appendix, after taking the massless limit for the electron and positron distribution. The final result is presented in eq. (D.12). It is then shown that in the limit of high Fermi momentum, we obtain the expression (cf. (D.13)):

$$
\begin{aligned}
(ap_0 + b)[p_0, |\mathbf{p}|] &= \frac{\alpha}{\pi} \frac{p_F^2}{2|\mathbf{p}|} \log \frac{p_0 - p}{p_0 + p} \\
a(p_0, |\mathbf{p}|) &= \frac{\alpha}{\pi} \frac{p_F^2}{\mathbf{p}^2} \left(1 + \frac{p_0}{2|\mathbf{p}|} \log \frac{p_0 - |\mathbf{p}|}{p_0 + |\mathbf{p}|} \right).
\end{aligned} \tag{5.20}
$$

Comparing this with results (C.10) and (C.12), we obtain the relation

$$
T \sim \frac{p_F}{\pi}. \tag{5.21}
$$

We know that the temperature of a gas of relativistic fermions is related to the fermion density by [28]

$$
n \propto \pi^2 T^3. \tag{5.22}
$$

On the other hand, we deduced in (5.5) that the density of a degenerate Fermi gas is given by

$$
n \propto \frac{p_F^3}{\pi^2}. \tag{5.23}
$$

By equating the densities of a the high-temperature plasma (5.22) and the degenerate plasma (5.23) we obtain exprssion (5.21). This reafirms the results obtained in the present chapter in comparison with those reviewed in Chap. 4.

Chapter 6

Conclusions

We studied the self-energy of an electron in a highly degenerate plasma of massive relativistic electrons to one-loop order in QED. The results have shown that the electrons acquire a thermal mass that scales with the Fermi momentum p_F of the distribution and the coupling constant.

The exact electron dispersion relation was analytically calculated by analytic integration, and the result was presented in an implicit form. This was then integrated numerically and plotted considering a value of $p_F = 200\, m_e$, a reasonable value for the particular case of a degenerate distribution of electrons in the core of a neutron star. in beta equilibrium conditions.

The plot of the dispersion relation function has shown the existence of four stable solutions. Namely, in addition to electron and positron excitations, we have found two more solutions that must be interpreted as hole and anti-hole excitations.

Furthermore, approximate expressions were derived for the thermal rest mass of each of the four excitations, to leading order in the Fermi momentum. We showed there is a difference between the thermal rest mass of electrons and holes, as well as between positrons and anti-holes. This is a specific feature of massive plasmas, not observed in previous studies regarding massless systems. In particular, the calculations of H. A. Weldon [7, 8] regarding a symmetric plasma of massless electrons and positrons revealed the emergence of collective modes corresponding to hole and anti-hole excitations. However, contrary to tour case, all four modes (electron, positron, hole and anti-hole) have the same thermal rest mass.

Moreover, for our system of degenerate electrons one observes that electrons and positrons have different dispersion relations, and the same is true for holes and anti-holes. This is an exclusive feature of asymmetric plasmas, where the symmetry between matter and antimatter is broken by the thermal medium.

Finally, the thermal dependence of our dispersion relation was directly compared with that obtained by Weldon. In the massless limit, our expressions were found to be in agreement with Weldon's results, after the necessary adaptations are performed.

The results obtained herein may be applied in future investigation of astrophysical systems with degenerate distributions of electrons of very high density. Namely, any significant change of the effective masses of electrons or positrons may alter the kinematics and rates of beta and inverse beta decays and associated neutrino emission rates.

Bibliography

[1] A. Abrikosov, L. Gorkov, and I. Dzyaloshinski. *Methods of Quantum Field Theory in Statistical Physics.* Prentice-Hall, Inc., Englewood Cliffs, N.J., 1963.

[2] Takeo Matsubara. A New Approach to Quantum-Statistical Mechanics. *Prog. Theor. Phys.*, 14(4):351–378, 1955. doi: 10.1143/PTP.14.351.

[3] E. S. Fradkin. Green's Function Method in Quantum Field Theory and Quantum Statistics. *Proc. Labedev Inst.*, 29(6), 1965.

[4] J.I. Kapusta and C. Gale. *Finite-Temperature Field Theory Principles and Applications.* Cambridge University Press, 2nd edition, 2006.

[5] M. le Bellac. *Thermal Field Theory.* Cambridge University Press, 1996.

[6] F. Gross. *Relativistic Quantum Mechanics and Field Theory.* Wiley-VCH Verlag GmbH & Co., Weinheim, 2nd edition, 2004.

[7] H Arthur Weldon. Effective fermion masses of order gT in high-temperature gauge theories with exact chiral invariance. *Phys. Rev. D*, 26(10):2789–2796, 1982. ISSN 05562821. doi: 10.1103/PhysRevD.26.2789.

[8] H. Arthur Weldon. Dynamical holes in the quark-gluon plasma. *Phys. Rev. D*, 40 (7):2410–2420, 1989. ISSN 05562821. doi: 10.1103/PhysRevD.40.2410.

[9] H Arthur Weldon. Structure of the Quark Propagator at High Temperature. *Phys. Rev. D*, 61:36003, 1999.

[10] Frithjof Karsch and Martin Lütgemeier. Deconfinement and chiral symmetry restoration in an SU(3) gauge theory with adjoint fermions. *Nucl. Phys. B*, 550 (1-2):449–464, 1999. ISSN 05503213. doi: 10.1016/S0550-3213(99)00129-7.

[11] H Arthur Weldon. Covariant calculations at finite temperature: The relativistic plasma. *Phys. Rev. D*, 26(6):1394–1407, 1982. ISSN 05562821. doi: 10.1103/PhysRevD.26.1394.

[12] O Kaczmarek, Frithjof Karsch, Masakiyo Kitazawa, and Wolfgang Söldner. Thermal mass and dispersion relations of quarks in the deconfined phase of quenched QCD. *Phys. Rev. D*, 86(036006), 2012.

[13] Rolf Hagedorn. Statistical thermodynamics of strong interactions at high energies. *Supp. N. Cim.*, 3(147), 1965.

[14] Helmut Satz. Deconfinement: concept, theory, test. In Jean Letessier, Hans H. Gutbrod, and Johann Rafelski, editors, *Hot Hadron. Matter – Theory Exp.*, pages 93–104. Springer, New York, 1995. ISBN 978-1-4613-5798-8.

[15] F. K. Thielemann, J. H. Applegate, J. J. Cowan, and M. Wiescher. Production of heavy elements in inhomogenous cosmologies. In H. Oberhummer, editor, *Nucl. Cosm.*, pages 147–177. Springer-Verlag, Berlin Heidelberg, 1991. ISBN 3-540-54198-5.

[16] N. Glendenning. *Compact Stars*. Springer, Heidelberg, 2nd edition, 2000. ISBN o 387 98977 3.

[17] A. Burrows. Neutrinos from Supernova Explosions. *Annu. Rev. Nucl. Part. Sci.*, 40:181–212, 1990.

[18] Alexander Fetter and John Dirk Walecka. *Quantum Theory of Many-Particle Systems*. McGraw-Hill, New York, 1971.

[19] J. W. Gibbs. *Elementary Principles in Statistical Mechanics*. Yale University Press, New Haven, 1902.

[20] O. Penrose. *Foundations of Statistical Mechanics*. Pergamon Press, 2005.

[21] L. E. Reichl. *A Modern Course in Statistical Physics*. John Wiley & Sons, 2nd edition, 1998.

[22] P. A. M. Dirac. *The Principles of Quantum Mechanics*. Oxford University Press, 1930.

[23] Steven Weinberg. Gauge and global symmetries at high temperature. *Phys. Rev. D1*, 9(12):3357–3378, 1979.

[24] J. M. Ziman. *Elements of Advanced Quantum Theory*. Cambridge University Press, 1969.

[25] C. Itzykson and J-B. Zuber. *Quantum Field Theory*. McGraw-Hill Education, 1980.

[26] E. Lifshitz L. Landau. *Statistical Physics*. Pergamon Press, 3rd edition, 1980.

[27] Charles Kittel. *Introduction to Solid State Physics*. John Wiley & Sons, New York, 7th edition, 1996.

[28] Kyriakos Tamvakis. An Introduction to the Physics of the Early Universe. In E. Papantonopoulos, editor, *Phys. Early Universe*, page 12. Springer-Verlag, Berlin Heidelberg, 2005.

Appendix A

Derivation of the Feynman propagator

In the following, we will show how one way of arriving at expression (2.11) for the free electron propagator. In spite of the ubuiquity of this propagator, and the fact that it has been derived in multiple ways in common literature on QED, we find that the specific procedure which we will follow here for its derivation is important for a better understanding of our study at finite-temperature, namely the concept of thermal propagators derived in §3.5.

We may write the definition of the free propagator (2.11) as

$$\begin{aligned} S^0(x) &= -\, i \left\langle 0 \middle| T\left[\psi(x)\bar{\psi}(0)\right] \middle| 0 \right\rangle \\ &= -\, i \left\langle 0 \middle| \left[\theta(t)\psi(x)\bar{\psi}(0) - \theta(-t)\bar{\psi}(0)\psi(x)\right] \middle| 0 \right\rangle \end{aligned} \tag{A.1}$$

We have used the homogeneity and isotropy of the system in order to write $S^0(x, x') = S^0(x - x')$ and then take $x' = 0$ without any loss of generality, and purely for simplicity of writing.

Although the explicit expression of the free fields ψ and $\bar{\psi}$ in coordinate space has already been presented, we will repeat it here for ease of consultation:

$$
\begin{aligned}
\psi(x) =& \sum_s \int \frac{d^3p}{(2\pi)^3 2E_p} \left(b_s(p) u_s(p) e^{-i(E_p t - \mathbf{p}\cdot\mathbf{x})} + d_s^\dagger(p) v_s(p) e^{i(E_p t - \mathbf{p}\cdot\mathbf{x})} \right), \\
\bar{\psi}(x) =& \sum_s \int \frac{d^3p}{(2\pi)^3 2E_p} \left(b_s^\dagger(p) \bar{u}_s(p) e^{-i(E_p t - \mathbf{p}\cdot\mathbf{x})} + d_s(p) \bar{v}_s(p) e^{i(E_p t - \mathbf{p}\cdot\mathbf{x})} \right).
\end{aligned}
\tag{A.2}
$$

We know that the destruction operators annihilate the ground state, as do the creation operators when applied from the right to the complex conjugate of the ground state:

$$
b\,|0\rangle = d\,|0\rangle = \langle 0|\, b^\dagger = \langle 0|\, d^\dagger = 0. \tag{A.3}
$$

After inserting in (A.1) the fields' internal structure (A.2) and distributing the product, we will get four terms, each containing a different pair of operators, but because of (A.3) it is easy to see that upon application to the ground state only two of these terms will survive, namely[1]

$$
S^0(x) = -i \sum_s \int \frac{d^3p}{(2\pi)^3 2E_p} \left\langle p, s \,\middle|\, \left[\theta(t) u_s \bar{u}_s e^{-ip\cdot x} - \theta(-t) \bar{v}_s v_s e^{ip\cdot x}\right] \,\middle|\, p, s \right\rangle,
$$

where $|p, s\rangle$ is the state occupied by one electron with momentum p and spin $s = \pm 1/2$. Next, we perform the sum over spins using then sum rules [6]

$$
\begin{aligned}
\sum_s u_s(p)\bar{u}_s(p) &= \not{p} + m \\
\sum_s v_s(p)\bar{v}_s(p) &= \not{p} - m,
\end{aligned}
\tag{A.4}
$$

and thus obtain

$$
S^0(x) = -i \int \frac{d^3p}{(2\pi)^3 2E_p} \left[\theta(t)(\not{p} + m) e^{-i(E_p t - \mathbf{p}\cdot\mathbf{x})} - \theta(-t)(\not{p} - m) e^{i(E_p t - \mathbf{p}\cdot\mathbf{x})}\right]. \tag{A.5}
$$

We will now introduce the following integral identity of the Heaviside theta function [6]:

[1] At finite temperature, on the other hand, the propagator involves the average over all possible states rather than just the ground state (cf. (3.17)), so that the other combinations of creation and annihilation operators will also partake, thus yielding twice as many degrees of freedom for the propagator.

$$\theta(t)e^{-iEt} = \frac{1}{2\pi i}\int dp_0 \frac{e^{-ip_0 t}}{E - p_0 - i\epsilon}. \tag{A.6}$$

Following [6], we may interpret this formula thusly: let us consider the p_0 complex plane. If we wish to perform a contour integral of a complex function of p_0 that includes the whole real axis, when we make the choice whether to close it through a semi-circle of radius $R \to \infty$ on the upper or the lower half-plane, we must choose the one in which the analytic function vanishes at infinity, otherwise we will get an infinite result. Now let us look at the RHS of (A.6). For $t > 0$, the factor $e^{-ip_0 t}$ allows us to close the integral only in the lower halp-plane; on the contrary, if $t < 0$, it is in the upper half-plane. But the function has a simple pole in the lower half-plane, at $p_0 = E - i\epsilon$. By the residue theorem, the contour integral will equal $2\pi i$ times the residue of the pole, which is e^{-iEt}, whenever the contour encloses the pole. Thus, the RHS will yield e^{-iEt} for $t > 0$, and zero for $t < 0$, which satisfies the definition of the theta function.

Substituting the theta function in the propagator by its integral form, we obtain

$$S^0(x) = -i\int \frac{d^3p}{(2\pi)^3 2E_p}\int \frac{dp_0}{2\pi i}\frac{(\not{p}+m)e^{-i(p_0 t - \mathbf{p}\cdot\mathbf{x})} - (\not{p}-m)e^{i(p_0 t - \mathbf{p}\cdot\mathbf{x})}}{E_p - p_0 - i\epsilon}. \tag{A.7}$$

We then change $(p_0, \mathbf{p}) \to -(p_0, \mathbf{p})$ in the second term:

$$\begin{aligned}
S^0(x) =& -i\int \frac{d^3p}{(2\pi)^3 2E_p}\int \frac{dp_0}{2\pi i}\Big[\frac{(\not{p}+m)e^{-ip\cdot x}}{E_p - p_0 - i\epsilon} + \frac{(\not{p}+m)e^{-ip\cdot x}}{E_p + p_0 - i\epsilon}\Big]e^{-i(p_0 t - \mathbf{p}\cdot\mathbf{x})} \\
=& -\int \frac{d^3p}{(2\pi)^3 2E_p}\int \frac{dp_0}{2\pi}(\not{p}+m)e^{-ip\cdot x}\left(\frac{2E_p}{E_p^2 - p_0^2 - i\epsilon}\right) \\
=& \int \frac{d^3p}{(2\pi)^3}\int \frac{dp_0}{2\pi}e^{-ip\cdot x}\left(\frac{\not{p}+m}{p_0^2 - E_p^2 + i\epsilon}\right) \\
=& \int \frac{d^3p}{(2\pi)^3}\int \frac{dp_0}{2\pi}e^{-ip\cdot x}S^0(p),
\end{aligned} \tag{A.8}$$

Where $S^0(p)$ is the Fourier transform of the propagator,

$$S^0(p) = \frac{\not{p}+m}{p_0^2 - E_p^2 + i\epsilon}, \tag{A.9}$$

which concludes our proof.

Appendix B

Perturbative expansion of the exact propagator at $T = 0$

In the present appendix we will explain the origin of the self-energy diagram at zero-temperature, by means of a brief survey on perturbation theory in QED as applied to the exact propagator.

As presented in §2.1, the exact single-electron QED propagator has a definite expression in the Heisenberg representation, namely

$$S(x,x') = -i \left\langle 0 \,\middle|\, T(\psi_H(x)\bar{\psi}_H(x')) \,\middle|\, 0 \right\rangle_H \tag{B.1}$$

This propagator cannot be calculated exactly; however, because in this theory the Hamiltonian may be separated into a free and an interaction term (cf. (2.1)),

$$\hat{H} = \hat{H}^0 + \hat{H}^{\text{int}}, \tag{B.2}$$

and if we consider the interaction energy to be small compared to the total energy of the system (which again is the case of QED, since we see from eq. (2.1) that $\hat{H}^{\text{int}}$ is proportional to the electron charge $e \ll 1$), then the interaction term may be treated as a perturbation. We then construct a series in $H^{\text{int}} \sim e$, where the unperturbed term is just the free propagator derived in the previous appendix:

$$\begin{aligned} S(x,x') =& S^0(x,x') + S^{(1)}(x,x') + S^{(2)}(x,x') + \cdots , \\ S^0(x,x') =& -i \left\langle 0 \,\middle|\, T(\psi(x)\bar{\psi}(x')) \,\middle|\, 0 \right\rangle , \end{aligned} \tag{B.3}$$

where the fields, now being in the interaction representation, are just the free particle solutions (2.7).

The key to calculating the Green's function (B.1) in such perturbative fashion is of course Wick's theorem. Insofar as this theorem is extensively described in standard field-theory literature [1, 6, 18], we shall neither prove it nor dwell on its formal details, but rather use directly the well-known result for the benefit of our conceptual discussion.

In order to enunciate properly that result, let us establish two definitions. The so-called *normal* product of operators is the following arrangement:

$$: aa^\dagger bb^\dagger \cdots : \; = (-1)^P a^\dagger b^\dagger \cdots ab \cdots \, , \tag{B.4}$$

where P is the number of permutations of fermionic operators. Basically, one places all the creation operators within the product on the left. Notice that a normal product of *any* sequence of operators will always yield zero expectation value in the ground state, $\langle 0 \,|\, : \; \cdots : \;|\, 0\rangle = 0$, and there resides the usefulness of the definition.

Let us further define the *contraction* (or 'pairing') of two operators (for instance ψ and $\bar{\psi}$):

$$\overbrace{\psi(x)\bar{\psi}(x')} = T\Big(\psi(x)\psi^\dagger(x')\Big) - : \psi(x)\psi^\dagger(x') : \tag{B.5}$$

Basically, we define the pairing as the term one must add when turning a time-ordered product of two operators into the normal order. At the same time we know that, by definition, the expectation value of any normal-ordered product in the ground state is zero; therefore, if we take the ground state expectation value of both sides of (B.5), it follows immediately that

$$\overbrace{\psi(x)\bar{\psi}(x')} = \Big\langle 0 \Big| \, T\Big(\psi(x)\psi^\dagger(x')\Big) \Big| 0 \Big\rangle \, . \tag{B.6}$$

Thus, the contraction of these fields simply corresponds to the free propagator, S^0.

Wick's theorem is simply the prescription for rearranging a time-ordered product of *any number* of operators into normal order. It states that in doing that rearrangement, one must then add their normal products with *all* possible combinations of contractions of the fields within. Symbolically[6],

$$
\begin{aligned}
T(\psi_1\cdots\psi_n) =&: \psi_1\cdots\psi_n : + : \overbracket{\psi_1\psi_2}\cdots\psi_n : + : \overbracket{\psi_1\psi_2\psi_3}\cdots\psi_n : + \cdots \\
&+ : \psi_1\overbracket{\psi_2\psi_3}\cdots\psi_n : + : \overbracket{\psi_1\psi_2}\overbracket{\psi_3\psi_4}\cdots\psi_n : + \cdots \\
&+ : \overbracket{\psi_1\psi_2}\overbracket{\psi_3\psi_4}\overbracket{\psi_5\psi_6}\cdots\psi_n : + \cdots
\end{aligned}
\tag{B.7}
$$

We will now apply Wick's theorem to the perturbative analysis of the QED interaction. It may be shown ([18] p. 85) that the series expansion of the exact propagator, represented above symbolically (B.3), may be given the form

$$
S(x,x') \propto \sum_{N=0}^{\infty} \frac{(-i)^{N+1}}{N!} \int dt_1 \cdots \int dt_N \left\langle 0 \middle| T\Big(\hat{H}^{\text{int}}(t_1)\cdots\hat{H}^{\text{int}}(t_N)\psi(x)\psi^\dagger(x')\Big) \middle| 0 \right\rangle
\tag{B.8}
$$

(where the operators, as well as the ground state, are in the interaction picture). We see that each term in the expansion (B.8) contains a time-ordered product involving only free fields and a successively increasing number of interaction Hamiltonians, themselves also containing free fields:

$$
H^{\text{int}} = \frac{1}{2}\int d\mathbf{x}_1 d\mathbf{x}_2 \psi^\dagger(\mathbf{x}_1)\psi^\dagger(\mathbf{x}_2)V(y-z)\psi(\mathbf{x}_2)\psi(\mathbf{x}_1)
\tag{B.9}
$$

Therefore, we may apply Wick's theorem to each term in the perturbative series. Let us exemplify with the term $S^{(1)}$, which immediately follows the unperturbed term. Inserting the expression of the interaction Hamiltonian, it may be written [1]

$$
S^{(1)}(x,x') \propto e^2 \int d^4x_1 d^4x_2 V(x_1-x_2) \left\langle 0 \middle| T\Big[\psi(x)\psi^\dagger(x')\psi^\dagger(x_1)\psi^\dagger(x_2)\psi(x_2)\psi(x_1)\Big] \middle| 0 \right\rangle
\tag{B.10}
$$

By using Wick's theorem (B.7), the time-ordered product in the integrand yields the sum

$$
\begin{aligned}
T\Big[\psi(x)\psi^\dagger(x')\psi^\dagger(x_1)\psi^\dagger(x_2)\psi(x_2)\psi(x_1)\Big] =& \overbracket{\psi(x)\psi^\dagger}(x')\psi^\dagger(x_1)\psi^\dagger(x_2)\psi(x_2)\psi(x_1) \\
&+\cdots
\end{aligned}
\tag{B.11}
$$

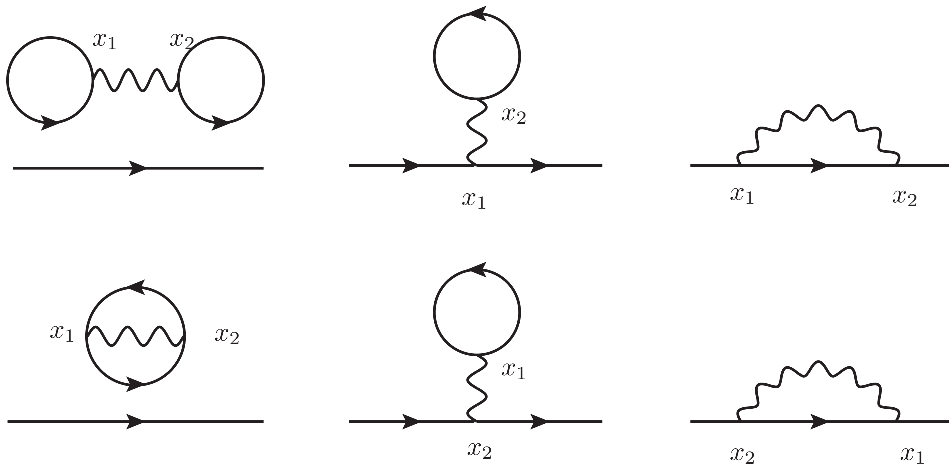

Figure B.1: Feynman diagrams of the second-order terms of the propagator expansion (B.11).

Each of the terms in (B.11) represents a contribution of second order of the propagator expansion, and each may be represented by a Feynman diagram. As we have shown, a contraction simply corresponds to a free particle propagator; this allows us to draw the diagram of each of these terms as shown in fig. B.1.

It may be shown [18] that the two leftmost diagrams, which are *disconnected*, factor out and cancel exactly with the overall denominator, which has been omitted so far, for simplicity. This cancelling happens to every order, and therefore we may disregard any term representing a disconnected diagram. Moreover, topologically identical diagrams that differ only in the space-time labelling of the vertices contribute equally, since x_1 and x_2 are to be integrated over all domain (cf. (B.10)). In that sense, the effect of these repeated diagrams is only to cancel the statistical factor $1/N!$ in each term of the series (cf. (B.8)). Thus, we are left with only two different second-order diagrams contributing to $G^{(1)}$.

Because the system is uniform and isotropic we may write $S(x, x') = S(x - x')$, and we are therefore able to perform a Fourier transform of the propagator into momentum space:

$$S(p) = \frac{1}{(2\pi)^4} \int d^4k e^{-ik\cdot(x-x')} S(x - x') \tag{B.12}$$

For this reason, the diagrams may be drawn in momentum space as represented in fig. B.2. These are the self-energy and tadpole diagrams discussed in §2.1.

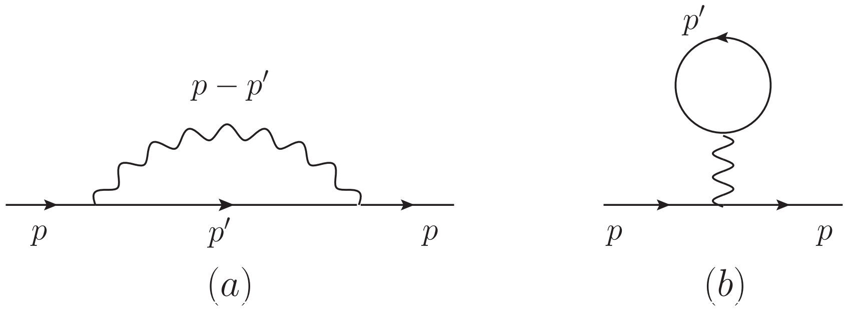

FIGURE B.2: Second-order diagrams that contribute to the propagator expansion. (a) Electron self-energy diagram (b) Tadpole diagram.

Appendix C

Calculation of the chirally invariant modes in a symmetric plasma

This appendix addresses the calculation of the modes yielded by the real, temperature-dependent part of the one-loop self-energy correction

$$\Sigma_\beta = -e^2 \int \frac{d^4p'}{4\pi^3} \frac{\not{p}'}{(p-p')^2} n_F(p')\delta(p'^2), \tag{C.1}$$

where free fermions are considered massless, and the Fermi-Dirac distribution is equal for electrons and positrons,

$$n_F(p', \beta) = \frac{1}{1+e^{\beta E_{p'}}}, \tag{C.2}$$

where $E_{p'}$ is the energy of the particles measured in the rest frame of the plasma. This corresponds to the system studied in [7, 8], with the difference that we will neglect the photon distribution $n_B(k, u)$, which amounts to considering a low photon density in the medium. These explicit calculations are not to be found in the references mentioned, which further justifies the need to discuss them in the present work.

The first step is to separate the delta function in (C.1), which has a double root, into two, using the fact that for a function $f(x)$ with roots x_i, we have

$$\delta[f(x)] = \sum_i \frac{\delta(x - x_i)}{\left|\frac{\partial g}{\partial x}\right|_{x=x_i}}$$
$$\implies \delta(p_0'^2 - \mathbf{p}'^2) = \frac{1}{2|\mathbf{p}'|}\left[\delta(p_0' - |\mathbf{p}'|) + \delta(p_0' + |\mathbf{p}'|)\right] \tag{C.3}$$

where the two simple delta functions correspond to the plasma electrons and positrons, respectively.

We may then perform the integral in p_0', which is trivial due to the delta functions, and then separate the spatial integral into a radial and an angular part, and integrate trivially over $d\phi$.

$$\begin{aligned}\Sigma_\beta =& -e^2 \int \frac{d^3p'}{8\pi^3}\frac{1}{|\mathbf{p}|}\not{p}'\Big[\frac{1}{p^2 - 2(p_0|\mathbf{p}'| - \mathbf{p}\cdot\mathbf{p}')} \\ &+ \frac{1}{p^2 - 2(-p_0|\mathbf{p}'| - \mathbf{p}\cdot\mathbf{p}')}\Big] n_F(|\mathbf{p}'|) \\ =& -\frac{e^2}{4\pi^2}\int_{-1}^{+1} d(\cos\theta)\int_0^\infty |\mathbf{p}'|d|\mathbf{p}'|\not{p}'\Big[\frac{1}{p^2 - 2|\mathbf{p}'|(p_0 - |\mathbf{p}|\cos\theta)} \\ &+ \frac{1}{p^2 + 2|\mathbf{p}'|(p_0 + |\mathbf{p}|\cos\theta)}\Big] n_F(|\mathbf{p}'|).\end{aligned} \tag{C.4}$$

In a chirally invariant medium Σ_β may be described by only two projections, namely $\operatorname{tr}\not{p}\Sigma_\beta$ and $\operatorname{tr}\not{u}\Sigma_\beta$. As we have discussed in §4.4, these may be combined in the following manner:

$$\begin{aligned} a &= \frac{1}{4p^2}\operatorname{tr}\{(\not{p} - p_0\not{u})\Sigma_\beta\} = -\frac{1}{4p^2}\operatorname{tr}\{(\mathbf{p}\cdot\boldsymbol{\gamma})\Sigma_\beta\} \\ ap_0 + b &= -\frac{1}{4}\operatorname{tr}\{\not{u}\Sigma_\beta\} = -\frac{1}{4}\operatorname{tr}\{\gamma_0\Sigma_\beta\},\end{aligned} \tag{C.5}$$

where a and b are the corrections to the dispersion relation that we want to calculate:

$$(1 + a)(p_0 \mp |\mathbf{p}|) + b = 0 \tag{C.6}$$

(cf. (4.12)). We will start with $ap_0 + b$. In what follows, we will use the identity $\operatorname{tr}\not{a}\not{b} = 4a\cdot b$:

$$
\begin{aligned}
ap_0 + b &= -\frac{1}{4}\operatorname{tr}\{\not{u}\Sigma_\beta\} \\
&= \left(\frac{e}{2\pi}\right)^2 \int\limits_{-1}^{+1} d(\cos\theta) \int\limits_0^\infty |\mathbf{p}'|d|\mathbf{p}'|p_0' \left[\frac{1}{p^2 - 2|\mathbf{p}'|(p_0 - |\mathbf{p}|\cos\theta)} + \frac{1}{p^2 + 2|\mathbf{p}'|(p_0 + |\mathbf{p}|\cos\theta)}\right] n_F(|\mathbf{p}'|) \\
&= \left(\frac{e}{2\pi}\right)^2 \int_0^\infty |\mathbf{p}'|d|\mathbf{p}'| \frac{p_0'}{2|\mathbf{p}||\mathbf{p}'|} \left[\log\frac{p^2 - 2|\mathbf{p}'|(p_0 - |\mathbf{p}|)}{p^2 - 2|\mathbf{p}'|(p_0 + |\mathbf{p}|)} + \log\frac{p^2 + 2|\mathbf{p}'|(p_0 + |\mathbf{p}|)}{p^2 + 2|\mathbf{p}'|(p_0 - |\mathbf{p}|)}\right] n_F(|\mathbf{p}'|) \\
&= \left(\frac{e}{2\pi}\right)^2 \frac{1}{2|\mathbf{p}|} \int_0^\infty |\mathbf{p}'|d|\mathbf{p}'| \left[\log\frac{p^2 - 2|\mathbf{p}'|(p_0 - |\mathbf{p}|)}{p^2 - 2|\mathbf{p}'|(p_0 + |\mathbf{p}|)} - \log\frac{p^2 + 2|\mathbf{p}'|(p_0 + |\mathbf{p}|)}{p^2 + 2|\mathbf{p}'|(p_0 - |\mathbf{p}|)}\right] n_F(|\mathbf{p}'|) \\
&= \left(\frac{e}{2\pi}\right)^2 \frac{1}{2|\mathbf{p}|} \int_0^\infty |\mathbf{p}'|d|\mathbf{p}'| \left[\log\frac{(p_0 - |\mathbf{p}|)(p_0 + |\mathbf{p}| - 2|\mathbf{p}'|)}{(p_0 + |\mathbf{p}|)(p_0 - |\mathbf{p}| - 2|\mathbf{p}'|)} - \log\frac{(p_0 + |\mathbf{p}|)(p_0 - |\mathbf{p}| + 2|\mathbf{p}'|)}{(p_0 - |\mathbf{p}|)(p_0 + |\mathbf{p}| + 2|\mathbf{p}'|)}\right] n_F(|\mathbf{p}'|) \\
&= \left(\frac{e}{2\pi}\right)^2 \frac{1}{2|\mathbf{p}|} \int_0^\infty |\mathbf{p}'|d|\mathbf{p}'| \left(\mathrm{L}_1(p_0, |\mathbf{p}|, |\mathbf{p}'|) + 2\log\frac{p_0 - |\mathbf{p}|}{p_0 + |\mathbf{p}|}\right) n_F(|\mathbf{p}'|), \qquad \text{(C.7)}
\end{aligned}
$$

where we have defined the logarithmic function L_1 (and will further define L_2) as[1]

$$\mathrm{L}_{1\,(2)}(p_0, |\mathbf{p}|, |\mathbf{p}'|) = \log\frac{p_0 + |\mathbf{p}| + 2|\mathbf{p}'|}{p_0 - |\mathbf{p}| + 2|\mathbf{p}'|} \mp \log\frac{p_0 + |\mathbf{p}| - 2|\mathbf{p}'|}{p_0 - |\mathbf{p}| - 2|\mathbf{p}'|}. \qquad \text{(C.8)}$$

We may now utilise the result

$$\int\limits_0^\infty p n_F(p) dp = \frac{\pi^2 T^2}{12}. \qquad \text{(C.9)}$$

Following [7], we note that for $p \gg p_0$ we have $\mathrm{L}_1 \to |\mathbf{p}|/|\mathbf{p}'|$, so that if there were no thermal distribution in the integrand of (C.7), the term proportional to $|\mathbf{p}'|\,\mathrm{L}_1(p_0, |\mathbf{p}|, |\mathbf{p}'|)$ would diverge only logarithmically, which allows us to drop it. We thus conclude that in the high-temperature approximation,

$$(ap_0 + b)[p_0, |\mathbf{p}|] \approx (eT)^2 \frac{1}{16|\mathbf{p}|} \log\frac{p_0 - |\mathbf{p}|}{p_0 + |\mathbf{p}|}. \qquad \text{(C.10)}$$

We now follow a similar procedure for a. Knowing that $\operatorname{tr}\{(\not{p} - p_0\not{u})\not{p}'\} = 4(p - u)\cdot p' = \mathbf{p}\cdot\mathbf{p}'$, it follows

[1] All logarithms are to be interpreted in the principle-value sense, as discussed in §4.3. In practice, this means considering the absolute value of the argument.

$$
\begin{aligned}
a &= \frac{1}{4p^2}\,\mathrm{tr}\{(\not{p} - p_0\not{u})\Sigma_\beta\} \\
&= \frac{e^2}{\mathbf{p}^2}\int_0^\infty \frac{d^4p'}{4\pi^3}\frac{\mathbf{p}\cdot\mathbf{p}'}{(p-p')^2}\frac{\delta(p_0'-\mathbf{p}')+\delta(p_0'+\mathbf{p}')}{2|\mathbf{p}'|}n_F(|\mathbf{p}'|) \\
&= \left(\frac{e}{2\pi}\right)^2\frac{1}{\mathbf{p}^2}\int_{-1}^{+1} d(\cos\theta)\int_0^\infty \frac{d^3p'}{8\pi^3}\frac{1}{|\mathbf{p}'|}|\mathbf{p}||\mathbf{p}'|\cos\theta\left[\frac{1}{p^2-2|\mathbf{p}'|(p_0-|\mathbf{p}|\cos\theta)}\right. \\
&\qquad\left. + \frac{1}{p^2+2|\mathbf{p}'|(p_0+|\mathbf{p}|\cos\theta)}\right]n_F(|\mathbf{p}'|) \\
&= \left(\frac{e}{2\pi}\right)^2\frac{1}{\mathbf{p}^2}\int_0^\infty |\mathbf{p}'|d|\mathbf{p}'|\left[1-\frac{|\mathbf{p}||\mathbf{p}'|(p^2-2p_0|\mathbf{p}'|)}{4\mathbf{p}^2\mathbf{p}'^2}\log\frac{p^2-2|\mathbf{p}'|(p_0-|\mathbf{p}|)}{p^2-2|\mathbf{p}'|(p_0+|\mathbf{p}|)}\right. \\
&\qquad\left. +1-\frac{|\mathbf{p}||\mathbf{p}'|(p^2+2p_0|\mathbf{p}'|)}{4\mathbf{p}^2\mathbf{p}'^2}\log\frac{p^2+2|\mathbf{p}'|(p_0+|\mathbf{p}|)}{p^2+2|\mathbf{p}'|(p_0-|\mathbf{p}|)}\right]n_F(|\mathbf{p}'|) \\
&= \left(\frac{e}{2\pi}\right)^2\frac{1}{\mathbf{p}^2}\int_0^\infty d|\mathbf{p}'|\left[2|\mathbf{p}'|+\frac{p^2}{4|\mathbf{p}|}L_1(p,|\mathbf{p}'|)+\frac{p_0}{2|\mathbf{p}|}|\mathbf{p}'|\left(L_2(p,|\mathbf{p}'|)+2\log\frac{p_0-|\mathbf{p}|}{p_0+|\mathbf{p}|}\right)\right]n_F(|\mathbf{p}'|)
\end{aligned}
\tag{C.11}
$$

Following the previous reasoning, and since at high $|\mathbf{p}'| \gg p_0, |\mathbf{p}|$ we have $L_2 \to -p_0|\mathbf{p}|/\mathbf{p}'^2$ [7], we drop both the L_1 and the L_2 terms, and again using (C.9) we obtain in the high temperature regime

$$
a(p_0,|\mathbf{p}|) \approx \frac{(eT)^2}{8\mathbf{p}^2}\left(1+\frac{p_0}{2|\mathbf{p}|}\log\frac{p_0-|\mathbf{p}|}{p_0+|\mathbf{p}|}\right). \tag{C.12}
$$

With the values of ap_0+b (C.10) and a (C.12), we may now calculate the dispersion relation (C.6) (albeit in an implicit form, because these parameters have logarithmic dependence on $p_0, |\mathbf{p}|$):

$$
p_0 \mp |\mathbf{p}|\left[1+\frac{(eT)^2}{8\mathbf{p}^2}\left(1+\frac{p_0}{2|\mathbf{p}|}\log\frac{p_0-|\mathbf{p}|}{p_0+|\mathbf{p}|}\right)\right]+(eT)^2\frac{1}{16|\mathbf{p}|}\log\frac{p_0-|\mathbf{p}|}{p_0+|\mathbf{p}|}=0. \tag{C.13}
$$

For $T \to 0$, as well as $|\mathbf{p}| \to \infty$, we retrieve the two solutions of the free Dirac equation, as expected.

The result of the numerical computation of (C.13) is presented in fig. 4.5.

Appendix D

Calculation of massive modes in a highly degenerate electron plasma

This appendix addresses the calculation of the dispersion relation of massive electrons rsulting from their self-energy interaction in a highly degenerate electron plasma of high Fermi momentum, $p_F \gg m$.

D.1 Development of the self-energy integrals

Using definitions (4.13) and (5.10), we obtain from the real part of the self-energy (5.13):

$$
\begin{aligned}
(ap_0 + b)[p_0, |\mathbf{p}|] &= -\frac{1}{4}\mathrm{tr}\left\{\not{u}\Sigma_\beta\right\} = \frac{e^2}{(2\pi)^3}\int d^3|\mathbf{p}'|\frac{1}{E_{p'}}\frac{E_{p'}}{(p-p')^2}\theta(p_F - |\mathbf{p}'|) \\
&= \left(\frac{e}{2\pi}\right)^2 \int_{-1}^{1} d\cos\theta \int_0^{p_F} d|\mathbf{p}'| \frac{\mathbf{p}'^2}{p^2 + m^2 - 2p_0E_{p'} + 2|\mathbf{p}||\mathbf{p}'|\cos\theta} \\
&= \left(\frac{\alpha}{\pi}\right)\int_0^{p_F} d|\mathbf{p}'|\frac{\mathbf{p}'^2}{2|\mathbf{p}||\mathbf{p}'|}\log\frac{p^2 + m^2 - 2p_0E_{p'} + 2|\mathbf{p}||\mathbf{p}'|}{p^2 + m^2 - 2p_0E_{p'} - 2|\mathbf{p}||\mathbf{p}'|} \\
&= \left(\frac{\alpha}{\pi}\right)\frac{1}{2|\mathbf{p}|}\int_0^{p_F} d|\mathbf{p}'||\mathbf{p}'|\log\frac{p^2 + m^2 - 2p_0E_{p'} + 2|\mathbf{p}||\mathbf{p}'|}{p^2 + m^2 - 2p_0E_{p'} - 2|\mathbf{p}||\mathbf{p}'|} \\
&= \left(\frac{\alpha}{\pi}\right)\frac{1}{2|\mathbf{p}|}\int_0^{p_F} d|\mathbf{p}'||\mathbf{p}'|\left[L(|\mathbf{p}'|, m, p_0 + |\mathbf{p}|) - L(|\mathbf{p}'|, m, p_0 - |\mathbf{p}|)\right]
\end{aligned}
$$

where we have defined

$$
\mathrm{L}(|\mathbf{p}'|, m, p_0 \pm |\mathbf{p}|) = \log\frac{p_0 \pm |\mathbf{p}| - E_{p'} - |\mathbf{p}'|}{p_0 \pm |\mathbf{p}| - E_{p'} + |\mathbf{p}'|}. \tag{D.1}
$$

As for the chirality-violating term c, one has

$$\begin{aligned}
c(p_0,|\mathbf{p}|) &= -\frac{1}{4}\mathrm{tr}\Sigma_\beta = -\left(\frac{e}{2\pi}\right)^2\int_{-1}^{1} d\cos\theta\int_0^{p_F} d|\mathbf{p}'|\mathbf{p}'^2\frac{1}{E_{p'}}\frac{2m}{p^2+m^2-2p_0E_{p'}+2|\mathbf{p}|\cdot|\mathbf{p}'|}\\
&= -\left(\frac{\alpha}{\pi}\right)2m\int_0^{p_F} d|\mathbf{p}'|\frac{\mathbf{p}'^2}{2|\mathbf{p}||\mathbf{p}'|E_{p'}}\log\frac{p^2+m^2-2p_0E_{p'}+2|\mathbf{p}||\mathbf{p}'|}{p^2+m^2-2p_0E_{p'}-2|\mathbf{p}||\mathbf{p}'|}\\
&= \left(\frac{\alpha}{\pi}\right)\frac{m}{|\mathbf{p}|}\int_0^{p_F} d|\mathbf{p}'|\frac{|\mathbf{p}'|}{E_{p'}}\log\frac{p^2+m^2-2p_0E_{p'}-2|\mathbf{p}||\mathbf{p}'|}{p^2+m^2-2p_0E_{p'}+2|\mathbf{p}||\mathbf{p}'|}\\
&= \left(\frac{\alpha}{\pi}\right)\frac{m}{|\mathbf{p}|}\int_0^{p_F} d|\mathbf{p}'|\frac{|\mathbf{p}'|}{E_{p'}}\left[\mathrm{L}(|\mathbf{p}'|,m,p_0-|\mathbf{p}|)-\mathrm{L}(|\mathbf{p}'|,m,p_0+|\mathbf{p}|)\right].
\end{aligned}$$

Using the previous definitions, we may write the spatial projection of the self-energy, a, in the following manner:

$$\begin{aligned}
a(p_0,|\mathbf{p}|) &= \frac{1}{\mathbf{p}^2}\frac{1}{4}\mathrm{tr}\left\{(\not p - p_0\not u)\Sigma_\beta\right\}\\
&= \frac{e^2}{\mathbf{p}^2}\int_0^{p_F}\frac{d^3|\mathbf{p}'|}{(2\pi)^3}\frac{1}{E_{p'}}\frac{|\mathbf{p}|\cdot|\mathbf{p}'|}{p^2+m^2-2p_0E_{p'}+2|\mathbf{p}||\mathbf{p}'|\cos\theta}\\
&= \left(\frac{e}{2\pi}\right)^2\frac{1}{\mathbf{p}^2}\int_{-1}^{1} d\cos\theta\int_0^{p_F} d|\mathbf{p}'|\mathbf{p}'^2\frac{1}{E_{p'}}\frac{|\mathbf{p}||\mathbf{p}'|\cos\theta}{p^2+m^2-2p_0E_{p'}+2|\mathbf{p}||\mathbf{p}'|\cos\theta}\\
&= \left(\frac{\alpha}{\pi}\right)\frac{1}{\mathbf{p}^2}\int_0^{p_F}\frac{d|\mathbf{p}'|\mathbf{p}'^2}{E_{p'}}\left[1-\frac{|\mathbf{p}||\mathbf{p}'|(p^2+m^2-2p_0E_{p'})}{4\mathbf{p}^2\mathbf{p}'^2}\log\frac{p^2+m^2-2(p_0E_{p'}-|\mathbf{p}||\mathbf{p}'|)}{p^2+m^2-2(p_0E_{p'}+|\mathbf{p}||\mathbf{p}'|)}\right]\\
&= \left(\frac{\alpha}{\pi}\right)\frac{1}{\mathbf{p}^2}\int d|\mathbf{p}'|\left[\frac{\mathbf{p}'^2}{E_{p'}}+\frac{|\mathbf{p}'|}{4|\mathbf{p}|E_{p'}}(p^2+m^2-2p_0E_{p'})\log\frac{p^2+m^2-2(p_0E_{p'}+|\mathbf{p}||\mathbf{p}'|)}{p^2+m^2-2(p_0E_{p'}-|\mathbf{p}||\mathbf{p}'|)}\right]\\
&\equiv \frac{1}{\mathbf{p}^2}\left\{\frac{p^2+m^2}{4m}\mathbf{c}(p_0,|\mathbf{p}|)+p_0[\mathbf{ap_0}+\mathbf{b}](p_0,|\mathbf{p}|)+\left(\frac{\alpha}{\pi}\right)\int_0^{p_F} d|\mathbf{p}'|\frac{\mathbf{p}'^2}{E_{p'}}\right\}\\
&= \frac{1}{\mathbf{p}^2}\left\{\frac{p^2+m^2}{4m}\mathbf{c}(p_0,|\mathbf{p}|)+p_0[\mathbf{ap_0}+\mathbf{b}](p_0,|\mathbf{p}|)+\frac{1}{2}\left(\frac{\alpha}{\pi}\right)\left(p_FE_F-m^2\log\frac{p_F+E_F}{m}\right)\right\}.
\end{aligned}$$

So that by calculating the time projection ap_0+b and the chirality-violating term c, we may then express a as a function of both.

D.2 Results obtained by analytic integration

The above integrals have been calculated analytically with the aid of *Mathematica*. This is possible due to the momentum cutoff at p_F arising from the degenerate distribution. The exact results are transcribed below.

$$\begin{aligned}
\frac{1}{\left(\frac{\alpha}{\pi}\right)}(ap_0+b)[p_0,|\mathbf{p}|] &= \frac{1}{16|\mathbf{p}|}\left\{\frac{[(p_0-|\mathbf{p}|-E_F)^2-p_F^2][(p_0-|\mathbf{p}|+E_F)^2-p_F^2]}{(p_0-|\mathbf{p}|)^2}\,\mathrm{L}(p_F,m,p_0-|\mathbf{p}|)\right.\\
&\quad\left.-\frac{[(p_0+|\mathbf{p}|-E_F)^2-p_F^2][(p_0+|\mathbf{p}|+E_F)^2-p_F^2]}{(p_0+|\mathbf{p}|)^2}\,\mathrm{L}(p_F,m,p_0+|\mathbf{p}|)\right\}\\
&\quad-\frac{p_0}{4}\left(\frac{m^2}{p^2}\right)^2\mathrm{L}(p_F,m,0)-\left(\frac{m^2}{p^2}+1\right)\frac{p_F}{4}\\
\frac{1}{\left(\frac{\alpha}{\pi}\right)}\frac{c(p_0,|\mathbf{p}|)}{m} &= \frac{1}{2|\mathbf{p}|}\left\{\frac{(p_0+|\mathbf{p}|-E_F)^2-p_F^2}{p_0+|\mathbf{p}|}\,\mathrm{L}(p_F,m,p_0+|\mathbf{p}|)\right.\\
&\quad\left.-\frac{(p_0-|\mathbf{p}|-E_F)^2-p_F^2}{p_0-|\mathbf{p}|}\,\mathrm{L}(p_F,m,p_0-|\mathbf{p}|)\right\}\\
&\quad+\left(\frac{m^2}{p^2}\right)\mathrm{L}(p_F,m,0)\\
a(p_0,|\mathbf{p}|) &= \frac{1}{\mathbf{p}^2}\left[\left(\frac{p^2+m^2}{4m}\right)c(p_0,|\mathbf{p}|)+p_0(ap_0+b)[p_0,|\mathbf{p}|]\right.\\
&\quad\left.+\frac{1}{2}\left(\frac{\alpha}{\pi}\right)\left(E_Fp_F-m^2\log\frac{E_F+p_F}{m}\right)\right], \qquad \text{(D.2)}
\end{aligned}$$

where as before, we have defined a in relation with the other parameters, and L is again defined by eq. (D.1):

$$\mathrm{L}(p_F,m,p_0\pm|\mathbf{p}|)=\log\frac{p_0\pm|\mathbf{p}|-E_F-p_F}{p_0\pm|\mathbf{p}|-E_F+p_F} \qquad \text{(D.3)}$$

The above expressions are exact results regarding the one-loop self-energy of a massive electron in a degenerate plasma of Fermi momentum p_F.

D.3 Rest energy of the fermionic modes

In the limit $p\to 0$, it is easy to show that the exact expressions obtained in the last section for ap_0+b, c and a become:

$$\frac{1}{\left(\frac{\alpha}{\pi}\right)}(ap_0+b)[p_0,|\mathbf{p}|\to 0] = -\frac{p_0}{4}\left\{\left(1-\frac{m^4}{p_0^4}\right)\mathrm{L}(p_F,m,p_0)+\frac{m^4}{p_0^4}\mathrm{L}(p_F,m,0)+2\frac{p_F}{p_0}\frac{p_0^2+m^2+p_0E_F}{p_0^2}\right\}$$

$$\frac{1}{\left(\frac{\alpha}{\pi}\right)}\frac{c(p_0,|\mathbf{p}|\to 0)}{m} = \left(1-\frac{m^2}{p_0^2}\right)\mathrm{L}(p_F,m,p_0)+\frac{m^2}{p_0^2}\mathrm{L}((p_F,m,0)+2\frac{p_F}{p_0}$$

$$a(p_0,|\mathbf{p}|\to 0) = -\frac{1}{4}\left(\frac{c(p_0,|\mathbf{p}|\to 0)}{m}\right) \tag{D.4}$$

Following def. (D.3), we have

$$\mathrm{L}(p_F,m,p_0)=\log\frac{p_0-E_F-p_F}{p_0-E_F+p_F}\xrightarrow{p_F\gg m}\log\frac{p_0-2p_F}{p_0}\xrightarrow{p_F\gg p_0}\log\frac{2p_F}{p_0}$$

$$\mathrm{L}(p_F,m,0)=\log\frac{E_F+p_F}{E_F-p_F}=\log\frac{(E_F+p_F)^2}{E_F^2-p_F^2}=2\log\frac{E_F+p_F}{m}\xrightarrow{p_F\gg m}2\log\frac{2p_F}{m}$$

Applying these approximations to expressions (D.4), we obtain

$$\frac{1}{\left(\frac{\alpha}{\pi}\right)}(ap_0+b)[p_0,|\mathbf{p}|\to 0] = -\frac{p_0}{4}\left\{\left(1-\frac{m^4}{p_0^4}\right)\log\frac{2p_F}{p_0}+2\frac{m^4}{p_0^4}\log\frac{2p_F}{m}+2\frac{p_F}{p_0}\frac{p_0^2+m^2+p_0p_F}{p_0^2}\right\}$$

$$\frac{1}{\left(\frac{\alpha}{\pi}\right)}\frac{c(p_0,|\mathbf{p}|\to 0)}{m} = \left(1-\frac{m^2}{p_0^2}\right)\log\frac{2p_F}{p_0}+2\frac{m^2}{p_0^2}\log\frac{2p_F}{m}+2\frac{p_F}{p_0}$$

$$a(p_0,|\mathbf{p}|\to 0) = -\frac{1}{4}\left(\frac{c(p_0,|\mathbf{p}|\to 0)}{m}\right) \tag{D.5}$$

These results are valid in the regime $p_F \gg m, p_0$. While the condition $p_F \gg m$ is naturally met for our systems of interest, the condition $p_F \gg p_0$ is suitable only for the estimation of the rest energy but fails for higher values of $|\mathbf{p}|$.

Substituting the approximate values (D.5) in the $|\mathbf{p}| = 0$ dispersion relation structure (5.15), we obtain the following approximate expression for the rest energy:

$$\mathcal{F}_{1\,(2)}(p_0, |\mathbf{p}| \to 0) \;=\; p_0 \mp m \;-\; \frac{\alpha}{\pi}\Bigg\{ p_F\left(\frac{p_F}{2p_0} - 2\frac{m}{p_0} + \frac{m^2}{2p_0^2} + \frac{1}{2}\right) + \left[\frac{m^3}{p_0^2}\left(\frac{m}{4p_0} \mp 1\right) \pm m - \frac{p_0}{4}\right]\log\frac{2p_F}{p_0} - \frac{m^3}{p_0^2}\left(\frac{m}{4p_0} \mp 1\right)\log\frac{2p_F}{m}\Bigg\} \;=\; 0 \qquad \text{(D.6)}$$

Note that the term in p_F^2 in the first line of (D.6) will be the leading-order correction; secondly, we have the terms proportional to p_F, also in the first line; the remaining corrections are all logarithmic in p_F and will therefore be the least relevant. So to leading order in p_F, the rest energy if the modes is given by

$$p_0 \mp m - \frac{\alpha}{2\pi}\frac{p_F^2}{p_0} = 0 \qquad \text{(D.7)}$$

This result corresponds to eq. (5.16) of §5.3.1.

D.4 Transformation into a positron plasma

It has been checked by explicit calculation that the self-energy functions a, b, c of an electron in a degenerate positron plasma may be obtained from those of an electron in a degenerate electron plasma (in §D.2) by performing the substitution $E_F,\, p_F \to -E_F,\, -p_F$. This yields

$$\frac{1}{\left(\frac{\alpha}{\pi}\right)}(ap_0 + b)[p_0, |\mathbf{p}|] \;=\; \frac{1}{16|\mathbf{p}|}\Bigg\{\frac{[(p_0 - |\mathbf{p}| - E_F)^2 - p_F^2][(p_0 - |\mathbf{p}| + E_F)^2 - p_F^2]}{(p_0 - |\mathbf{p}|)^2}\overline{\mathrm{L}}(p_F, m, p_0 - |\mathbf{p}|) - \frac{[(p_0 + |\mathbf{p}| - E_F)^2 - p_F^2][(p_0 + |\mathbf{p}| + E_F)^2 - p_F^2]}{(p_0 + |\mathbf{p}|)^2}\overline{\mathrm{L}}(p_F, m, p_0 + |\mathbf{p}|)\Bigg\} - \frac{p_0}{4}\left(\frac{m^2}{p^2}\right)^2 \mathrm{L}(p_F, m, 0) + \left(\frac{m^2}{p^2} + 1\right)\frac{p_F}{4}$$

$$\frac{1}{\left(\frac{\alpha}{\pi}\right)}\frac{c(p_0, |\mathbf{p}|)}{m} \;=\; \frac{1}{2|\mathbf{p}|}\Bigg\{\frac{(p_0 + |\mathbf{p}| - E_F)^2 - p_F^2}{p_0 + |\mathbf{p}|}\,\mathrm{L}(p_F, m, p_0 + |\mathbf{p}|) - \frac{(p_0 - |\mathbf{p}| - E_F)^2 - p_F^2}{p_0 - |\mathbf{p}|}\overline{\mathrm{L}}(p_F, m, p_0 - |\mathbf{p}|)\Bigg\} + \left(\frac{m^2}{p^2}\right)\overline{\mathrm{L}}(p_F, m, 0)$$

$$a(p_0,|\mathbf{p}|) = \frac{1}{\mathbf{p}^2}\left[\left(\frac{p^2+m^2}{4m}\right)c(p_0,|\mathbf{p}|)+p_0(ap_0+b)[p_0,|\mathbf{p}|] + \frac{1}{2}\left(\frac{\alpha}{\pi}\right)\left(E_F p_F - m^2\log\frac{E_F+p_F}{m}\right)\right], \tag{D.8}$$

where we have defined

$$\overline{\mathrm{L}}(p_F,m,p_0\pm|\mathbf{p}|) = \log\frac{p_0\pm|\mathbf{p}|+E_F+p_F}{p_0\pm|\mathbf{p}|+E_F-p_F}. \tag{D.9}$$

D.5 Self-energy in a symmetric, degenerate plasma of massless electrons and positrons

In order to compare our results for the electron self-energy in a degenerate electron plasma with those reviewed in Chap. 4, we must adapt them to the case of a symmetric, degenerate plasma of massless electrons and positrons. For that purpose, we take the massless limit of the self-energy functions for an electron in a degenerate electron plasma (D.2) and of those for an electron in a degenerate positron plasma (D.8), and sum both contributions[1]. The massless limit of (D.2) is

$$\begin{aligned}
\frac{1}{\left(\frac{\alpha}{\pi}\right)}(ap_0+b)[p_0,|\mathbf{p}|] &= \frac{1}{16|\mathbf{p}|}\Bigg\{\left[(p_0-|\mathbf{p}|)^2-4p_F^2\right]\log\frac{p_0-|\mathbf{p}|-2p_F}{p_0-|\mathbf{p}|} \\
&\quad - \left[(p_0+|\mathbf{p}|)^2-4p_F^2\right]\log\frac{p_0+|\mathbf{p}|-2p_F}{p_0+|\mathbf{p}|} - \frac{p_F}{4}\Bigg\} \\
a(p_0,|\mathbf{p}|) &= \frac{1}{\mathbf{p}^2}\left[\frac{p^2}{4}\left(\frac{c(p_0,|\mathbf{p}|)}{m}\right)+p_0(ap_0+b)[p_0,|\mathbf{p}|]+\frac{\alpha}{\pi}p_F^2\right] \\
\frac{1}{\left(\frac{\alpha}{\pi}\right)}\frac{c(p_0,|\mathbf{p}|)}{m} &= \frac{1}{2|\mathbf{p}|}\left[(p_0+|\mathbf{p}|-2p_F)\log\frac{p_0+|\mathbf{p}|-2p_F}{p_0+|\mathbf{p}|}-(p_0-|\mathbf{p}|-2p_F)\log\frac{p_0-|\mathbf{p}|-2p_F}{p_0-|\mathbf{p}|}\right]
\end{aligned} \tag{D.10}$$

This gives the self-energy of a massless electron in a degenerate plasma of massless electrons. Note that the function c does not enter the dispersion relation of a massless electron eqrefdispersion; however, c/m enters our expression of function a and must therefore be calculated.

Moreover, the massless limit of (D.8) is

[1] It has been checked by explicit calculation that this is in fact the correct procedure.

$$\begin{aligned}
\frac{1}{\left(\frac{\alpha}{\pi}\right)}(ap_0+b)[p_0,|\mathbf{p}|] &= \frac{1}{16|\mathbf{p}|}\Bigg\{\left[(p_0-|\mathbf{p}|)^2-4p_F^2\right]\log\frac{p_0-|\mathbf{p}|-2p_F}{p_0-|\mathbf{p}|} \\
&\quad -\left[(p_0+|\mathbf{p}|)^2-4p_F^2\right]\log\frac{p_0+|\mathbf{p}|-2p_F}{p_0+|\mathbf{p}|}-\frac{p_F}{4}\Bigg\} \\
a(p_0,|\mathbf{p}|) &= \frac{1}{\mathbf{p}^2}\left[\frac{p^2}{4}\left(\frac{c(p_0,|\mathbf{p}|)}{m}\right)+p_0(ap_0+b)[p_0,|\mathbf{p}|]+\frac{\alpha}{\pi}p_F^2\right] \\
\frac{1}{\left(\frac{\alpha}{\pi}\right)}\frac{c(p_0,|\mathbf{p}|)}{m} &= \frac{1}{2|\mathbf{p}|}\left[(p_0+|\mathbf{p}|-2p_F)\log\frac{p_0+|\mathbf{p}|-2p_F}{p_0+|\mathbf{p}|}-(p_0-|\mathbf{p}|-2p_F)\log\frac{p_0-|\mathbf{p}|-2p_F}{p_0-|\mathbf{p}|}\right],
\end{aligned} \tag{D.11}$$

which is the self-energy of a massless electron in a degenerate plasma of massless positrons. Putting together both contributions by summing solutions (D.10) and (D.11), we obtain the self-energy functions of an electron in a degenerate symmetric plasma of massless electrons and positrons:

$$\begin{aligned}
\frac{1}{\left(\frac{\alpha}{\pi}\right)}(ap_0+b)[p_0,|\mathbf{p}|] &= \frac{1}{16|\mathbf{p}|}\Bigg\{\left[(p_0-|\mathbf{p}|)^2-4p_F^2\right]\left[\log\frac{p_0-|\mathbf{p}|-2p_F}{p_0-|\mathbf{p}|}+\log\frac{p_0-|\mathbf{p}|+2p_F}{p_0-|\mathbf{p}|}\right] \\
&\quad -\left[(p_0+|\mathbf{p}|)^2-4p_F^2\right]\left[\log\frac{p_0+|\mathbf{p}|+2p_F}{p_0+|\mathbf{p}|}+\log\frac{p_0+|\mathbf{p}|-2p_F}{p_0+|\mathbf{p}|}\right]\Bigg\} \\
a(p_0,|\mathbf{p}|) &= \frac{1}{\mathbf{p}^2}\left[\frac{p^2}{4}\left(\frac{c(p_0,|\mathbf{p}|)}{m}\right)+p_0(ap_0+b)[p_0,|\mathbf{p}|]+\frac{\alpha}{\pi}p_F^2\right] \\
\frac{1}{\left(\frac{\alpha}{\pi}\right)}\frac{c(p_0,|\mathbf{p}|)}{m} &= \frac{1}{2|\mathbf{p}|}\Bigg[(p_0+|\mathbf{p}|-2p_F)\log\frac{p_0+|\mathbf{p}|-2p_F}{p_0+|\mathbf{p}|}+(p_0+|\mathbf{p}|-2p_F)\log\frac{p_0+|\mathbf{p}|-2p_F}{p_0+|\mathbf{p}|} \\
&\quad -(p_0-|\mathbf{p}|-2p_F)\log\frac{p_0-|\mathbf{p}|-2p_F}{p_0-|\mathbf{p}|}-(p_0-|\mathbf{p}|+2p_F)\log\frac{p_0-|\mathbf{p}|+2p_F}{p_0-|\mathbf{p}|}\Bigg].
\end{aligned} \tag{D.12}$$

In the regime of high Fermi momentum, the terms in p_F^2 will dominate; keeping only these contributions in the above expressions, the following approximations are obtained straightforwardly:

$$
\begin{aligned}
(ap_0+b)[p_0,|\mathbf{p}|] &= \frac{\alpha}{\pi}\frac{p_F^2}{4|\mathbf{p}|}\log\frac{(p_0+|\mathbf{p}|-2p_F)(p_0+|\mathbf{p}|+2p_F)(p_0-|\mathbf{p}|)^2}{(p_0-|\mathbf{p}|-2p_F)(p_0-|\mathbf{p}|+2p_F)(p_0+|\mathbf{p}|)^2} \\
&= \frac{\alpha}{\pi}\frac{p_F^2}{4|\mathbf{p}|}\left[2\log\frac{p_0-|\mathbf{p}|}{p_0+|\mathbf{p}|}+\log\frac{(p_0+|\mathbf{p}|)^2-4p_F^2}{(p_0-|\mathbf{p}|)^2-4p_F^2}\right] \\
&= \frac{\alpha}{\pi}\frac{p_F^2}{2|\mathbf{p}|}\log\frac{p_0-p}{p_0+p} \qquad\qquad (p_F\gg p_0,|\mathbf{p}|) \\
a(p_0,|\mathbf{p}|) &= \frac{p_0}{\mathbf{p}^2}\left(\frac{\alpha}{\pi}\frac{1}{2|\mathbf{p}|}p_F^2\log\frac{p_0-|\mathbf{p}|}{p_0+|\mathbf{p}|}\right)+\frac{\alpha}{\pi}\frac{p_F^2}{\mathbf{p}^2} \\
&= \frac{\alpha}{\pi}\frac{p_F^2}{\mathbf{p}^2}\left(1+\frac{p_0}{2|\mathbf{p}|}\log\frac{p_0-|\mathbf{p}|}{p_0+|\mathbf{p}|}\right) \qquad (p_F\gg p_0,|\mathbf{p}|) \qquad \text{(D.13)}
\end{aligned}
$$

In §5.3.3 the above expressions are compared and found to be consistent with those for a high-temperature symmetric plasma, (C.10) and (C.12).